INORGANIC NANOPARTICLES IN SELF-ORGANIZED BIOPOLYMER COMPLEXES AND SELF-ASSEMBLED COMPOSITE NANOBIOFILMS

Gennady B. Khomutov

Biophysics Department, Faculty of Physics, Moscow State University

Institute of General and Inorganic Chemistry RAS

Institute of Radioelectronics and Engineering RAS

Cambridge Nanolytic Ltd., Tetra Consult Ltd., ……

NANOSCIENCE 2009, 15-17 October 2009

Convergence of Nanoscience and Bioscience

Bioscience for Nanoscience and Technology:

Functional biomimetic systems and processes (self-organization, self-assembly, biomineralization (organic matrix-controlled formation of nanophase inorganic compounds and nanocomposites at normal ecologically-friendly conditions at low costs).

Nanoscience for Bioscience:

New techniques and methods for structural and functional studies with improved spatial resolution down to the nano-scale and high sensitivity (SPM, electron microscopy; electrons, X-rays, neutrons diffraction, spectroscopic and optical techniques, etc.). Nano-instrumentation and nanofabrication methods, new synthetic nanomaterials for bio-applications (biochips, microfluidics, nanoparticulate diagnostic, therapy and drug delivery tools, etc.).

Bioscience and Nanoscience together:

Novel bioactive or biocompatible hybrid systems and composite nanomaterials with new structural organization, properties and functionalities. Integration of biological structures and systems into novel devices, functional and information (intellectual?) systems and new materials or vice versa.

Current applications of inorganic nanoparticles in Biology and Medicine:

Noble metal nanoparticles.

Labeling, detection, bactericidal materials and coatings, therapy.
Biomolecule-noble metal nanoparticle conjugates are applicable for diagnostics and analytics using optical or electrical detection techniques.
Nanowires and networks formed via DNA metallization.

Semiconductor nanoparticles.

Labeling, detection, self-cleaning surfaces.

Magnetic nanoparticles, generally, Iron oxide nanoparticles.

Biogenic and synthetic magnetic iron oxide nanoparticles (usually superparamagnetic due to their small size) with appropriate surface modification and functionalization have been used in magnetic resonance imaging contrast enhancement, magnetic detection of biomolecular interactions and bioassays, preparation of magnetic gels, biocompatible films, anti-cancer agents and targeting hyperthermia, targetable drug delivery and gene delivery (magnetic transfection) with carrier localization in a specific area, magnetic separation, analyses of DNA, cell labeling.

Natural magnetic bio-inorganic nanostructures

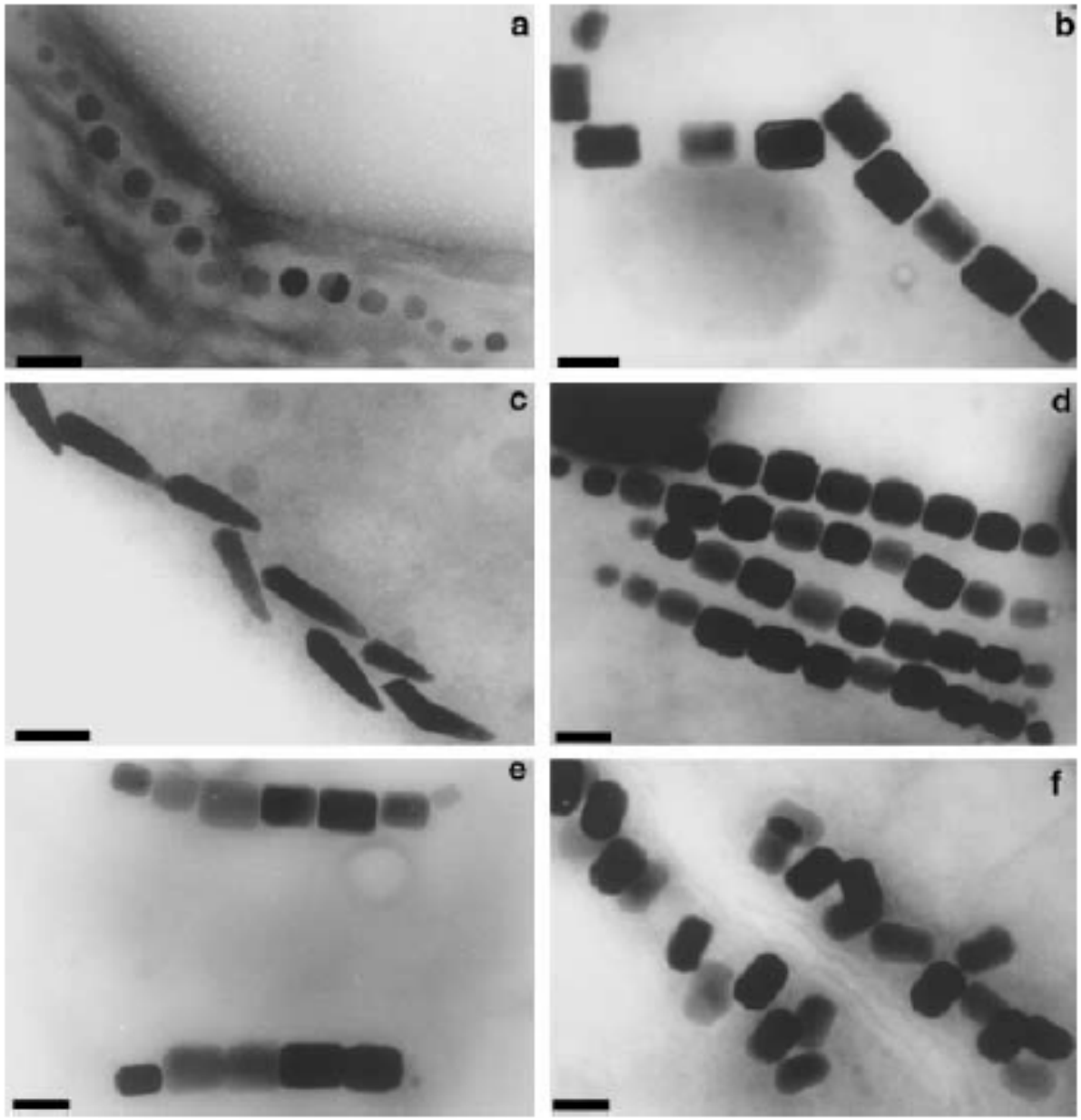

Transmission electron micrographs showing organized chain-like ensembles of magnetite Fe_3O_4 nanoparticles in magnetosomes of various Magnetotactic bacteria

Bar is equal to 100 nm

<u>From:</u> D. Schuler, R.B. Frankel, Appl. Nicrobiol. Biotechnol. 52 (1999) 464.

Aims of the work:

Investigation of basic physical-chemical mechanisms of ordered structure formation processes and structure-function relationships at the nano-scale level in various systems including biological, organic, inorganic and hybrid systems and related processes at the gas-liquid and liquid-solid interfaces.

The search of possibilities for practical applications of obtained results and for development of innovation products (intellectual property).
More than 20 patents now.

Methods

Synthetic “bottom-up” methods based on chemical reactions and physical interactions in a bulkk phase and at the gas-liquid interface, Langmuir-Blodgett technique, Layer-by-Layer self-assembly method, ligands exchange and substitution, integration and combination of nano-components of various nature, biomimetic strategies, self-assembling and self-organization principles, DNA templating and scaffolding.

Scanning Tunneling Microscopy and Spectroscopy

Atomic Force Microscopy

Transmission Electron Microscopy

Electron Paramagnetic Resonance

Optical spectroscopy

X-rays diffraction

Electron diffraction

Outline:

1. **Biomimetic nanoelectronic nanosystems:**
   single-electron tunneling and "flash" memory devices based on biomimetic system "redox metalloprotein in a membrane": organized planar nanocluster structures formed using Langmuir-Blodgett technique.

2. **Immobilized DNA complexes with amphiphilic polycations and intercalating dye formed using Langmuir-Blodgett technique.**

3. **Organized arrays of inorganic semiconductor (CdS, CdSe) and iron oxide nanoparticles formed using planar DNA complexes with amphiphilic polycation and intercalating dye.**

4. **Iron oxide nanoparticulate structures synthesized using ferritin as an iron source in immobilized DNA complexes.**

5. **Novel self-assembled free-standing magnetic nanocomposite nanobiofilms formed in a bulk aqueous phase without any surfaces and interfaces.**

5. **Conclusions**

1. Biomimetic approach to formation of regular nanolayer nanocomposites: Langmuir-Blodgett films with incorporated nano-components

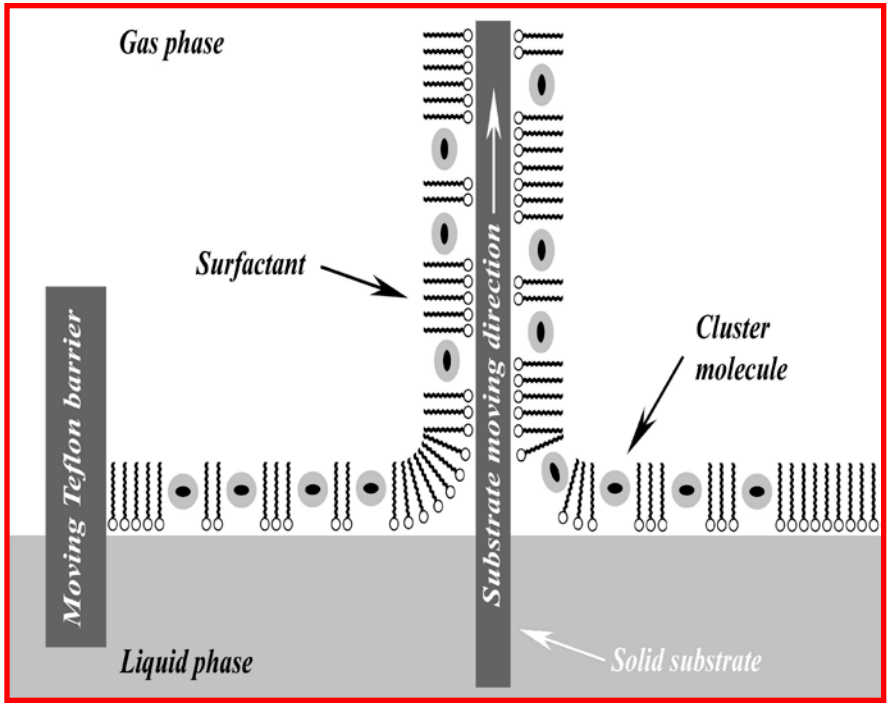

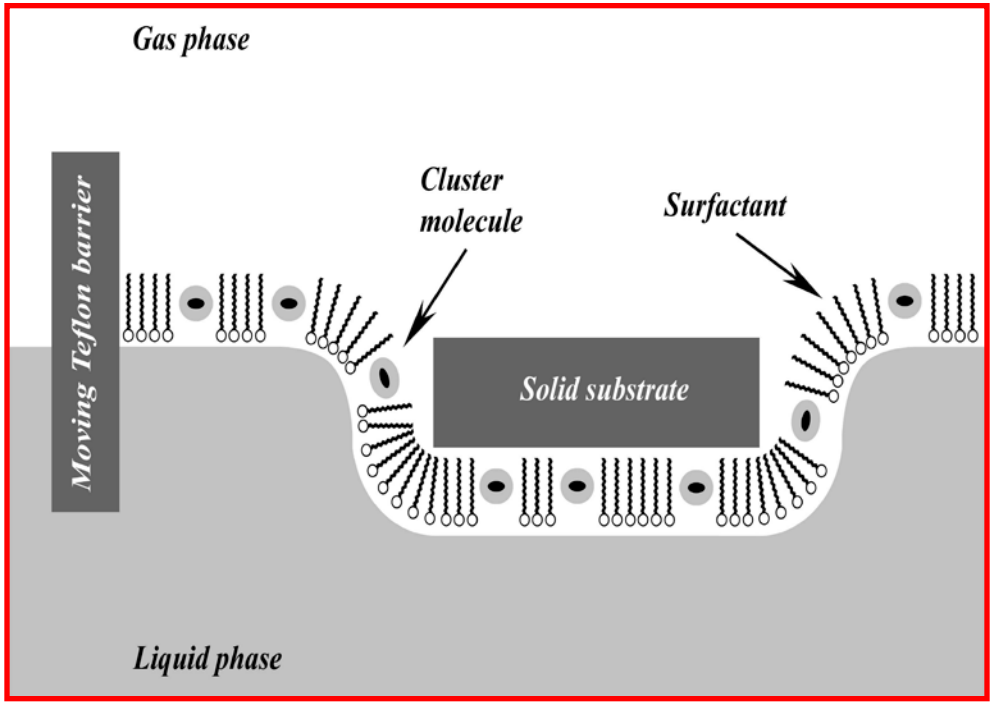

Vertical solid substrate lifting deposition technique (Langmuir-Blodgett method)

Horizontal solid substrate lifting deposition technique (Langmuir-Scheffer's method)

Investigated clusters and biomolecules

Chemical formula	Contour & size
Ferritin	sphere, 15 nm
Cytochrome c	sphere, 3 nm
Fulleren, C_{60}	sphere, 0.71 nm
Tl carboran, $1.7\text{-}(CH_3)_2\text{-}1.2\text{-}C_2B_{10}H_9Tl(OCOCF_3)_2$	1´ 1.4 nm
Carboran, $C_2B_{10}H_{12}$	0.7´ 0.7 nm
$Pt_3(CO)_3[P(C_2H_5)_3]_4$	torus, 1.5´ 0.6 nm
$Pt_4(CO)_5[P(C_2H_5)_3]_4$	1.3´ 1.1 nm
$Pt_5(CO)_5[P(C_2H_5)_3]_4$	1.3´ 1.1 nm
$Pt_5(CO)_6[P(C_2H_5)_3]_4$	ellipsoid, 1.3´ 1.1 nm
$Pt_5(CO)_7(P(C_6H_5)_3)_4$	1.3´ 1.1 nm
$Pt_{17}(CO)_{12}(P(C_2H_5)_3)_8$	2´ 0.8 nm
$Pd_3(CO)_3[P(C_6H_5)_3]_4$	torus, 1.5´ 0.6 nm
$Pd_{10}(CO)_{12}[P(C_4H_7)_3]_6$	sphere, 1.8 nm
$Pd_{23}(CO)_{20}[P(C_2H_5)_3]_8$	2.5´ 2.5 nm
$(C_5H_5)_4Fe_4S_4$	sphere, 7´ 7 nm
$[Fe_6C(CO)_{16}]^{2-} + 2´ [(C_2H_5)_4N]^{+1}$	0.9´ 0.9 nm
$Au_{101}(PPh_3)_{21}Cl_5$	core 2´ 2nm

STM topographic images of cluster molecule monolayers

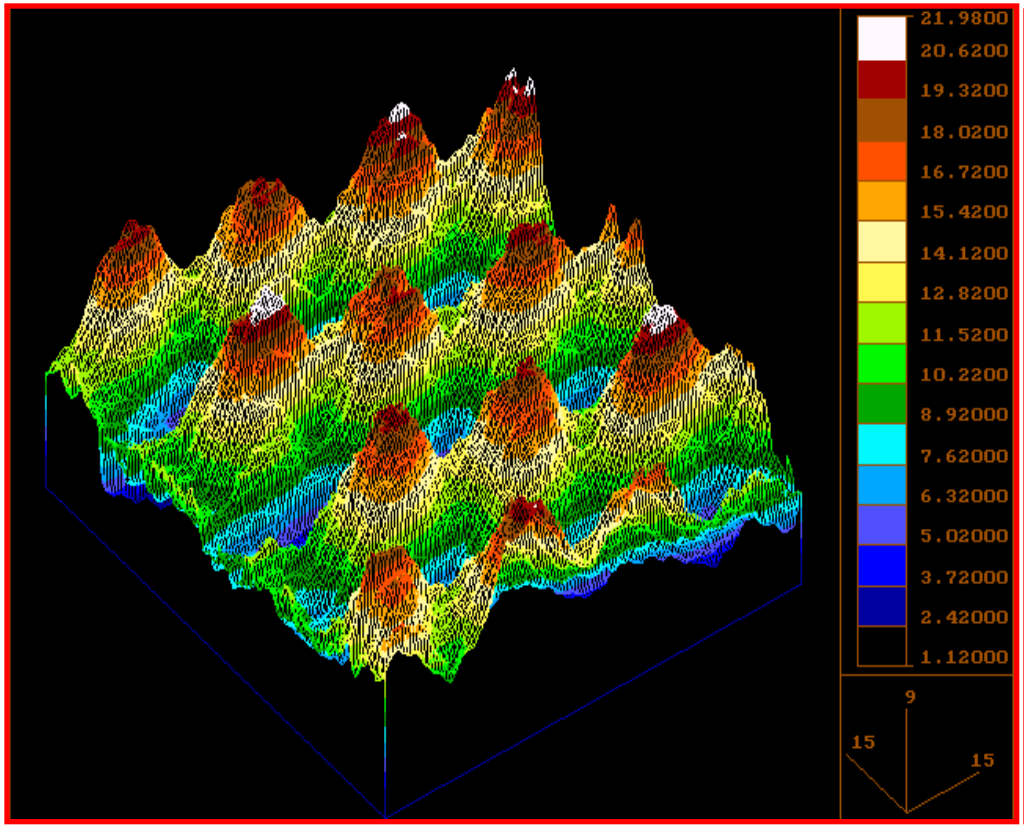

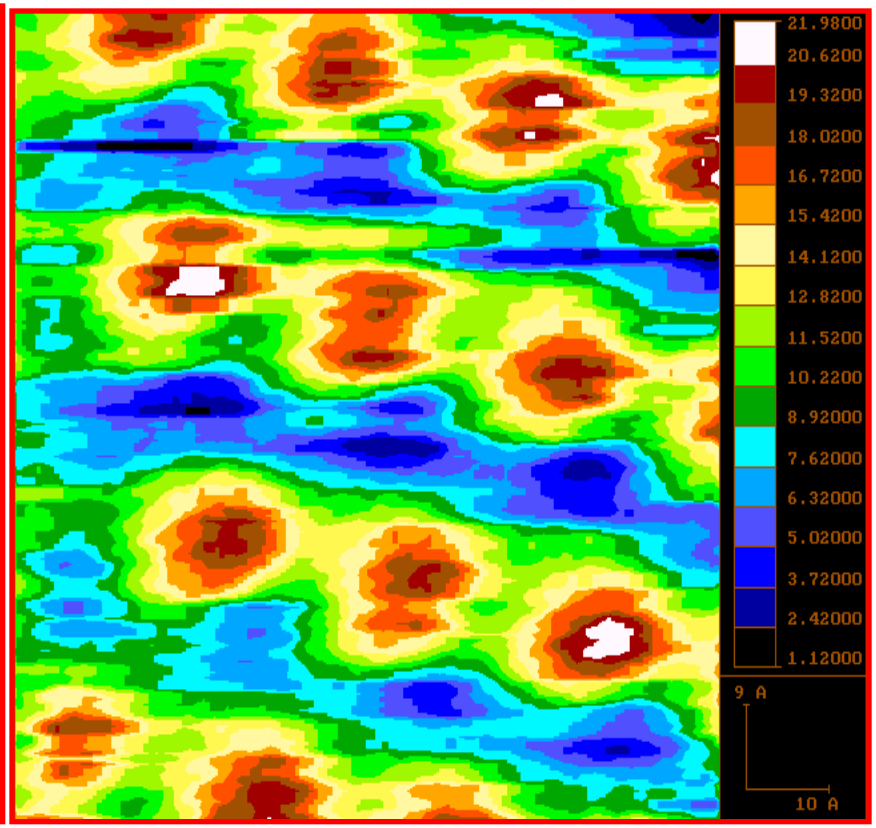

STM topographic images of carborane $C_2B_{10}H_{12}$ cluster molecule monolayer deposited by horizontal substrate lifting method onto the surface of HOPG substrate.

Temperature 21 ^{o}C, ambient conditions.

STM topographic image of Langmuir monolayer of $Au_{101}(PPh_3)_{21}Cl_5$ clusters

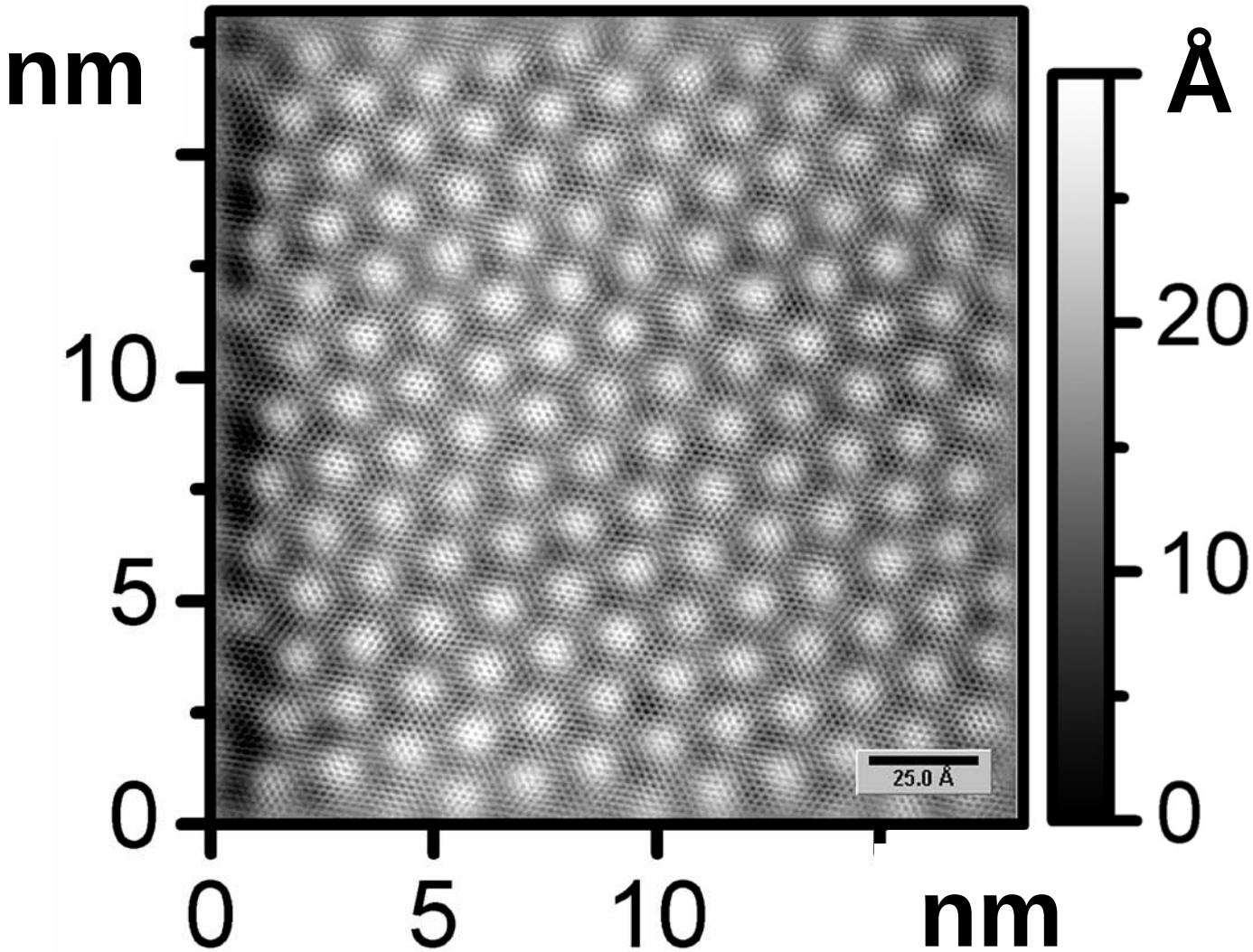

Langmuir monolayer of $Au_{101}(PPh_3)_{21}Cl_5$ clusters

was formed on water surface and deposited on HOP Graphite substrate by the horizontal substrate lifting deposition technique. The STM image was measured at room temperature.

First demonstration of single-molecule single-electron tunneling transistor working at ambient conditions

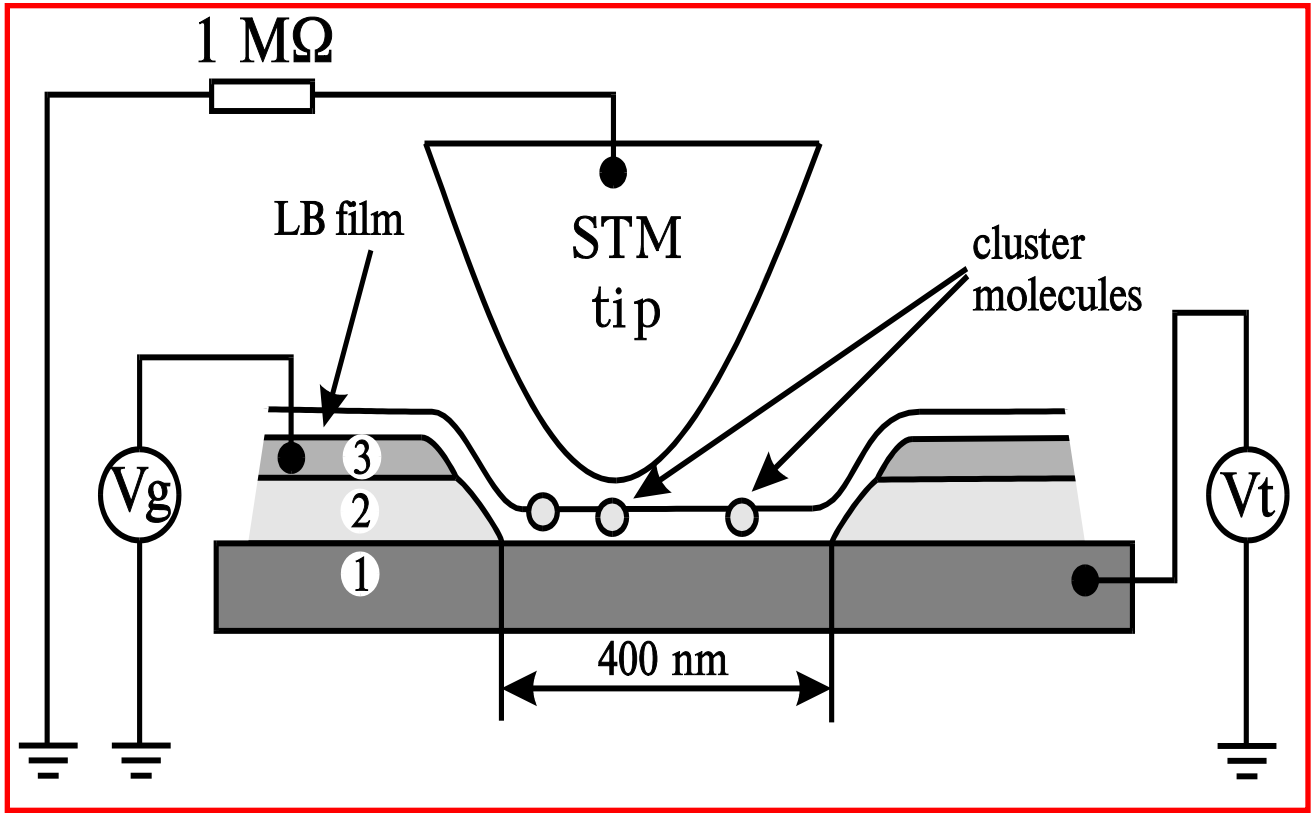

Schematic arrangement of the tunnel transistor system on the base of the single nanocluster molecule and STM with Au gate electrode

1 - HOPG

2 - Al_2O_3

3 - Au

From: E.S. Soldatov, V.V. Khanin, A.S. Trifonov, D.E. Presnov, S.A. Yakovenko, S.P. Gubin, V.V. Kolesov and G.B. Khomutov, *JETP Lett.*, 64 (1996) 556.

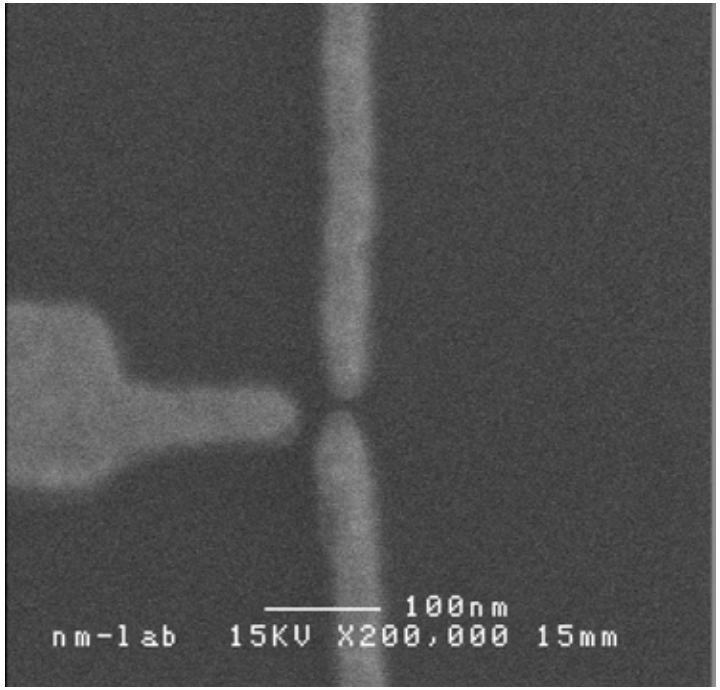

Scanning electron micrograph of nanoelectrodes from 20nm Au/5 nm Ti.

Patents:

RU 2105386, publication date 20.02.1998.
RU 2106041, publication date 27.02.1998.
PCT WO/1997/036333, publication date 02.10.1997.
US6057556, publication date 02.05.2000.
EP0836232, publication date 15.04.1998.
DE69721929, publication date 18.06.2003.
JP11500583, publication date 12.01.1999.
KR100272702, publication date 15.11.2000.
AU2579297, publication date 17.10.1997.
CN1189921, publication date 05.08.1998.

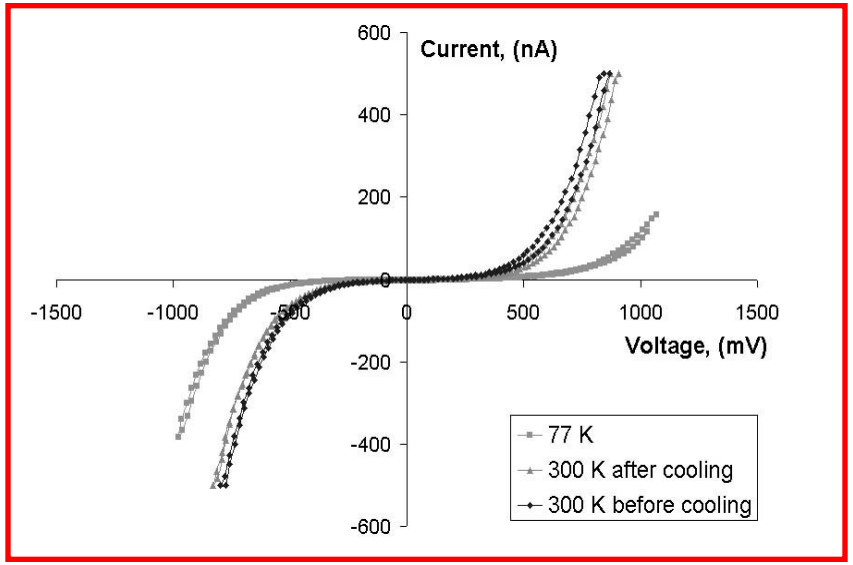

Typical tunnel current - bias voltage characteristics measured in planar nanoelectrodes system at various temperatures

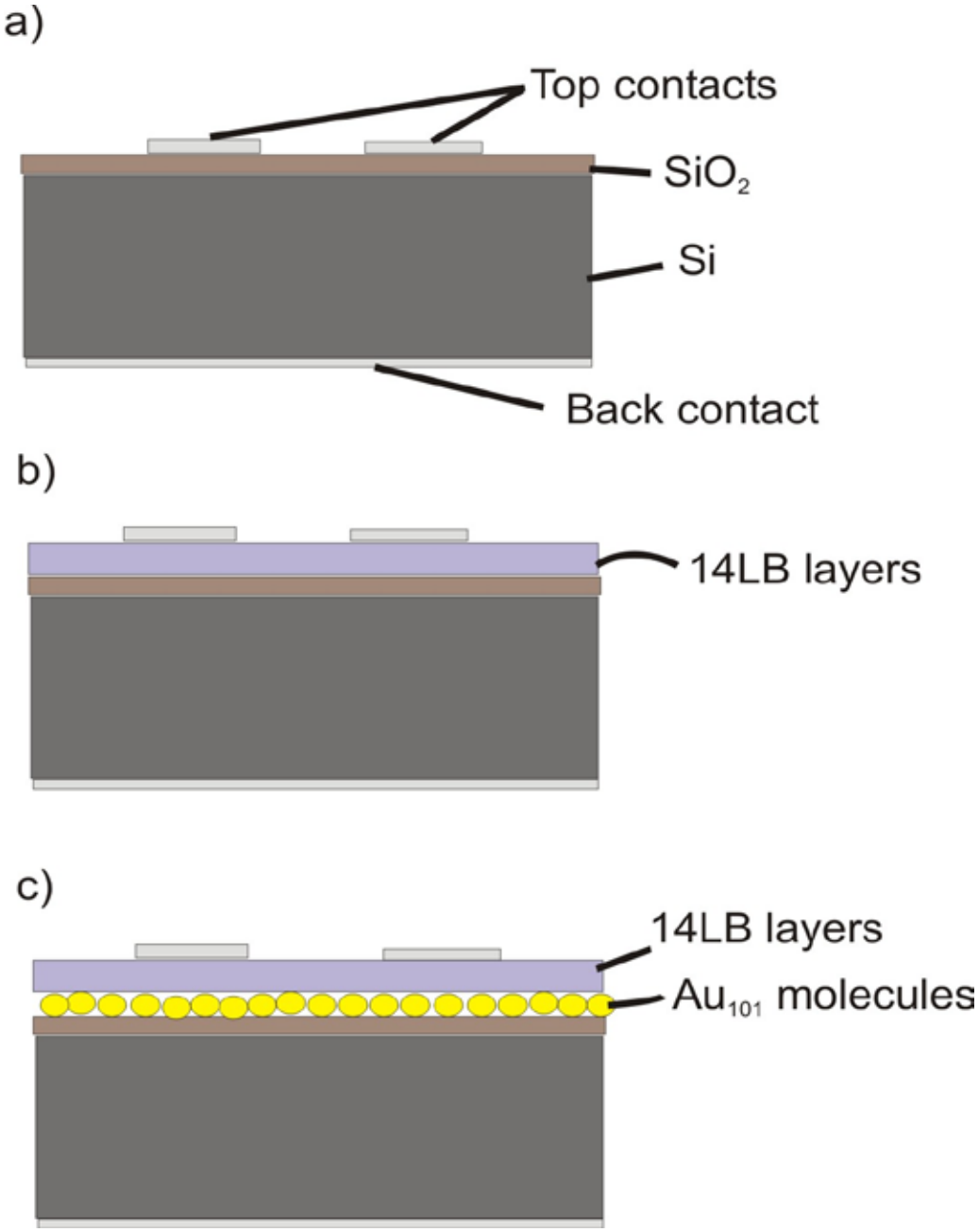

Schematic diagrams of construction elements of molecular nanocluster based floating gate memory device

a): Si/SiO_2 layer.

b): Si/SiO_2 layer/14 layers Langmuir-Blodgett film (Cd Arachidate or amphiphilic polyelectrolyte).

c): Si/SiO_2 layer/ $Au_{101}(PPh_3)_{21}Cl_5$ monolayer/14 layers Langmuir-Blodgett film.

Molecular nanocluster based floating gate memory device

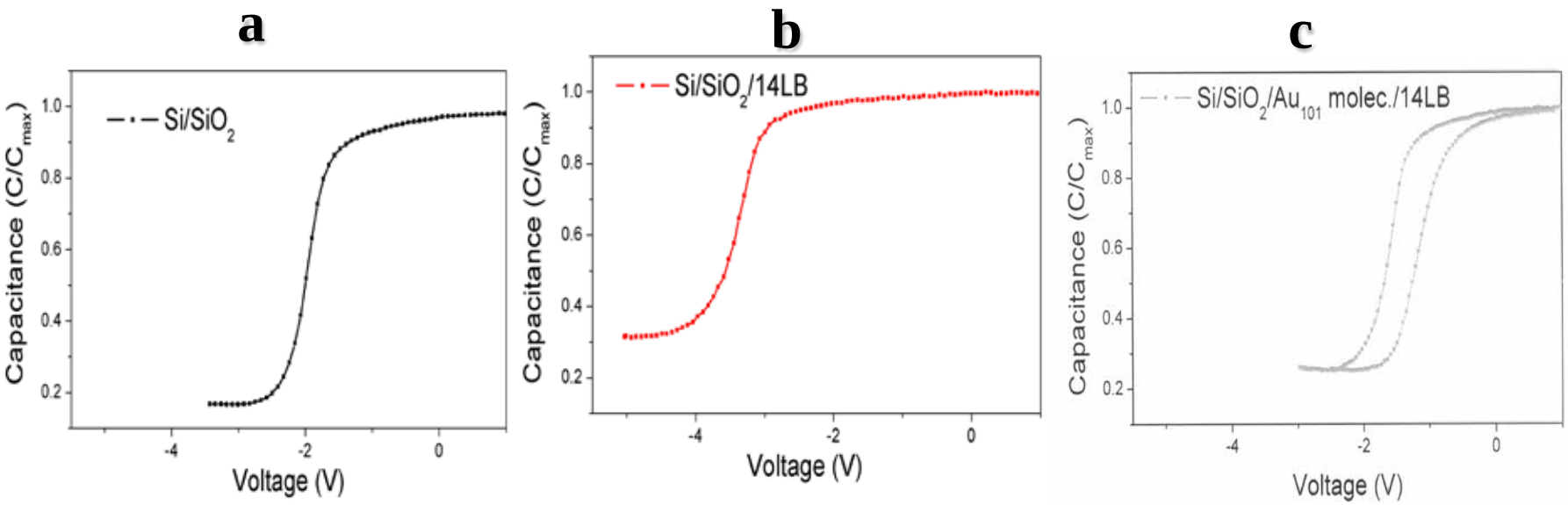

Normalized C-V curves of the samples:

a): Si/SiO_2 layer.

b): Si/SiO_2 layer/14 layers Langmuir-Blodgett film (Cd Arachidate or amphiphilic polyelectrolyte).

c): Si/SiO_2 layer/$Au_{101}(PPh_3)_{21}Cl_5$ monolayer/14 layers Langmuir-Blodgett film.

2. AFM characterization of interfacially-organized amphiphilic polyelectrolyte monolayer film

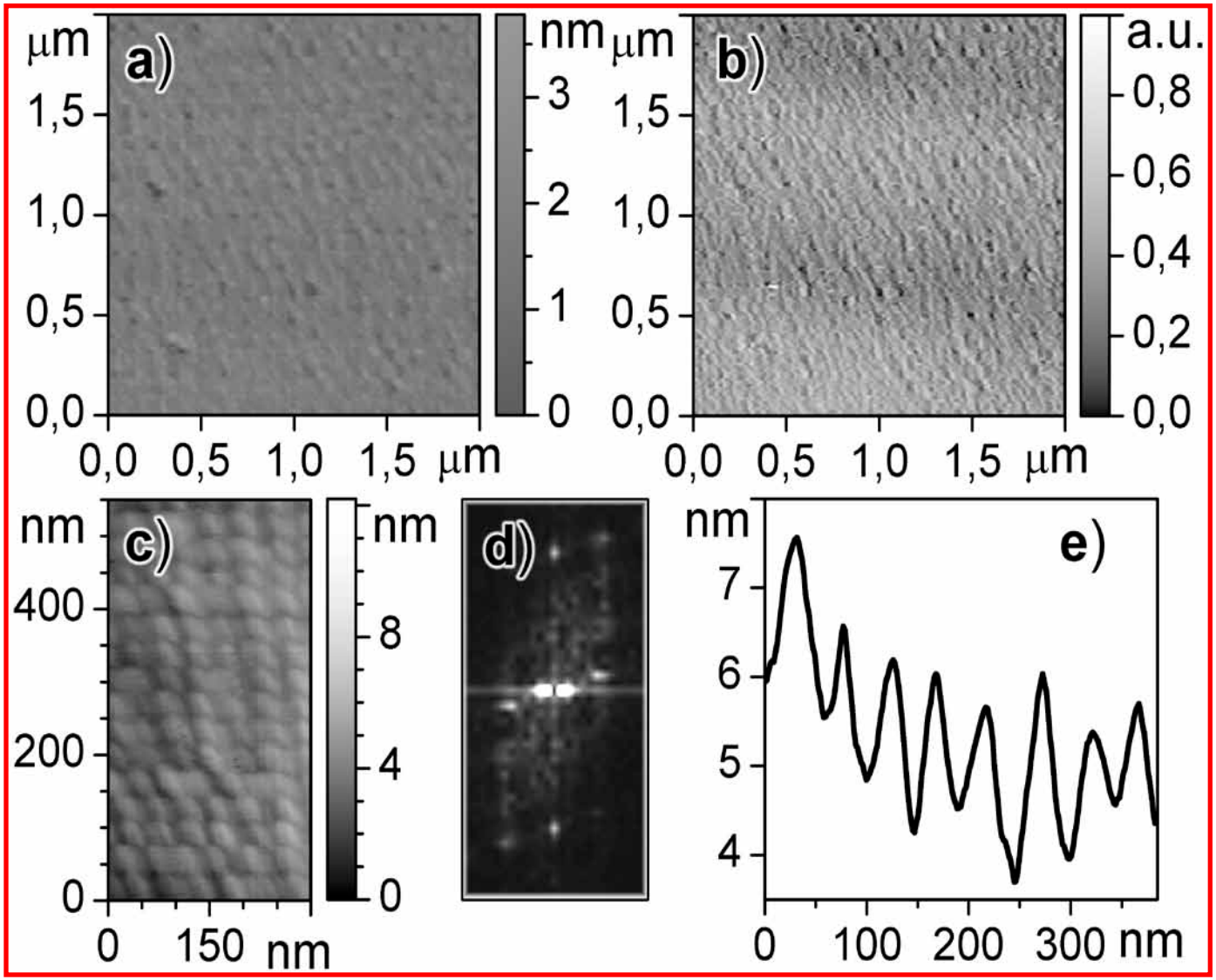

AFM tapping mode images of monolayer Langmuir-Blodgett film of water-insoluble amphiphilic polycation poly-4-vinylpyridine with 16% cationic cetylpyridinium groups (PVP-16) deposited onto the mica substrate after 10 min incubation of the PVP-16 Langmuir monolayer at low surface pressure value (p @) on the water subphase (pH=6);

<u>Images a) and b):</u> top view topographic images (black-to-white color height scale is 0-13 nm).

<u>Image c):</u> Fast Fourier analyses of the image a).

<u>Curve d):</u> Characteristic cross-section profile of the image a) parallel to the X-axis.

Poly-4-vinilpyridine with X% cetylpyridinium groups (PVP-X)

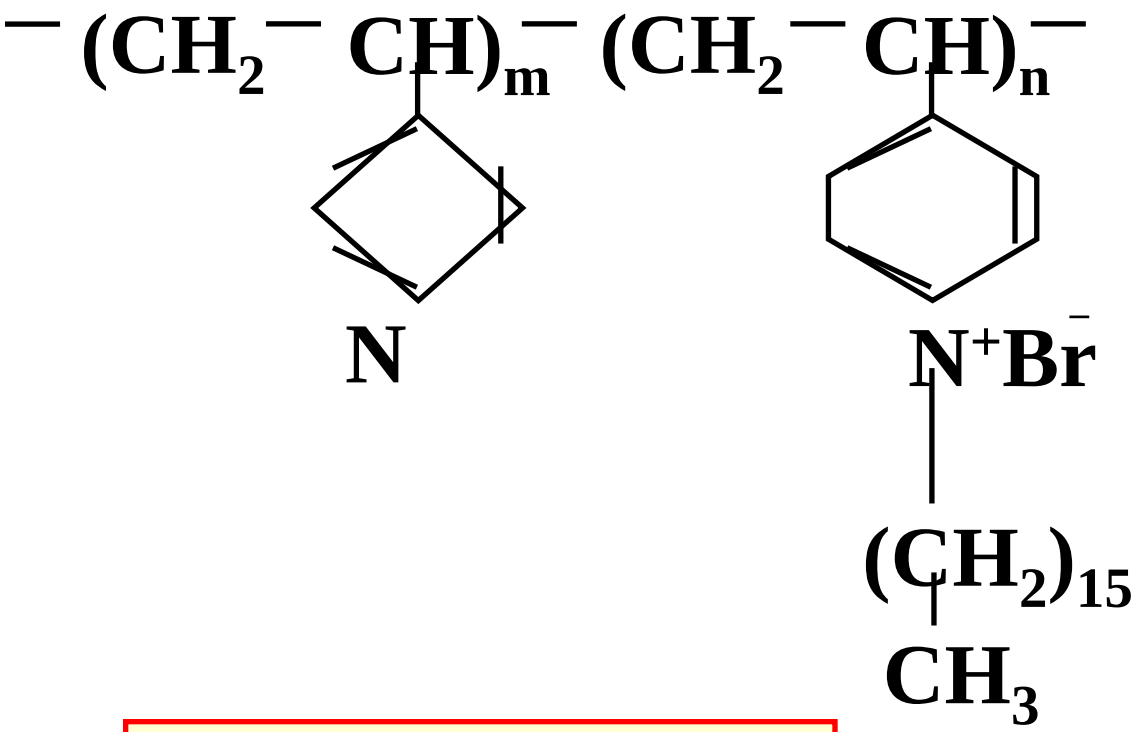

$$X = n/(m+n) \times 100\%$$

AFM tapping mode images of 2-layer LB films on mica substrate

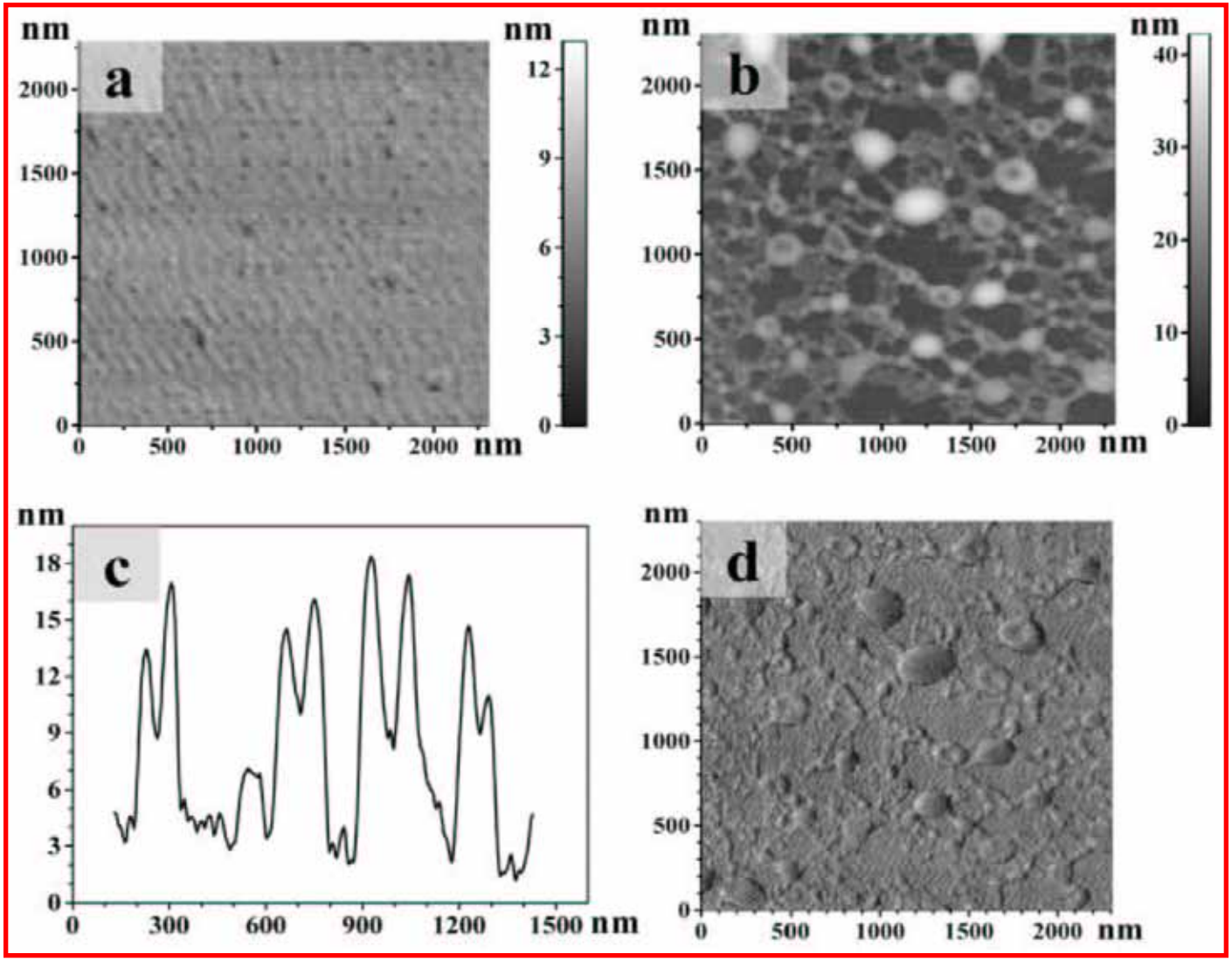

Image a): top view topographic image of PVP-16 LB film.
Image b): top view topographic images of DNA/PVP-16 complex LB film. Toroidal complex formation conditions: PVP-16 monolayer surface pressure value 20 mN/m during the DNA binding, incubation time 25 min on the surface of aqueous subphase with composition: 1,2´ 10^{-4} M DNA (for monomer), 1 mM NaCl, pH=6.
Curve c): characteristic cross-section profile of the image b) parallel to the X-axis.
Image d): AFM phase contrast mode top view image corresponding to the image b).

AFM tapping mode top view topographic images of DNA/PVP-16 complex 2-layer LB film

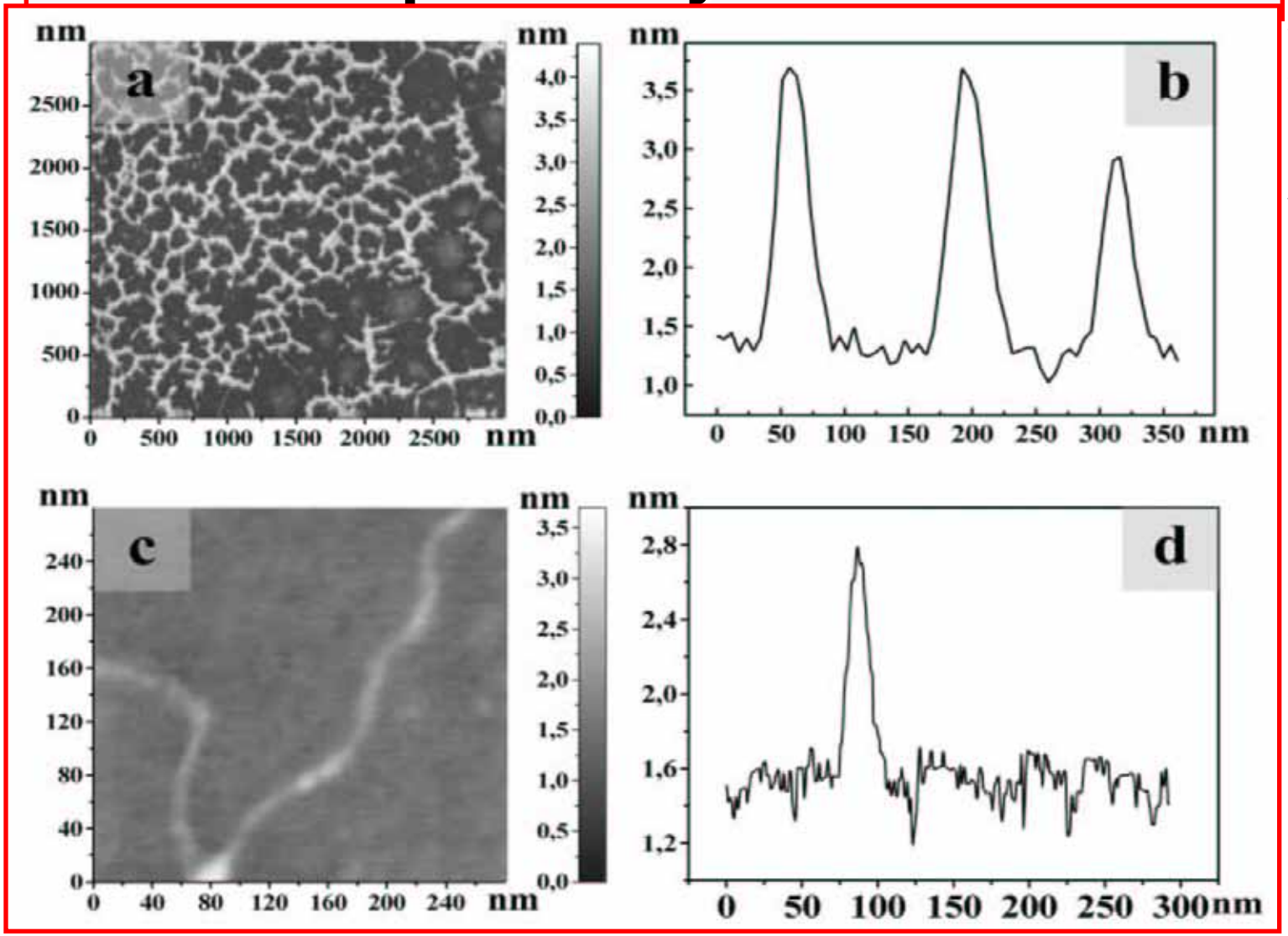

Complex formation conditions: PVP-16 monolayer surface pressure value ~ 0 during the DNA binding, incubation time 25 min. The composition of the aqueous subphase was 1,2´ 10^{-4} M DNA (for monomer), 1 mM NaCl, pH=6.

<u>Image a):</u> image size 3000 nm ´ 3000 nm.

<u>Curve b):</u> characteristic cross-section profile of the image a).

<u>Image c):</u> single DNA molecule bound with PVP-16 monolayer, image size: 280 nm ´ 280 nm.

<u>Curve d):</u> characteristic cross-section profile of the image c).

3. TEM micrographs showing iron oxide and CdS nanostructures grown in DNA/PVP-16 complexes

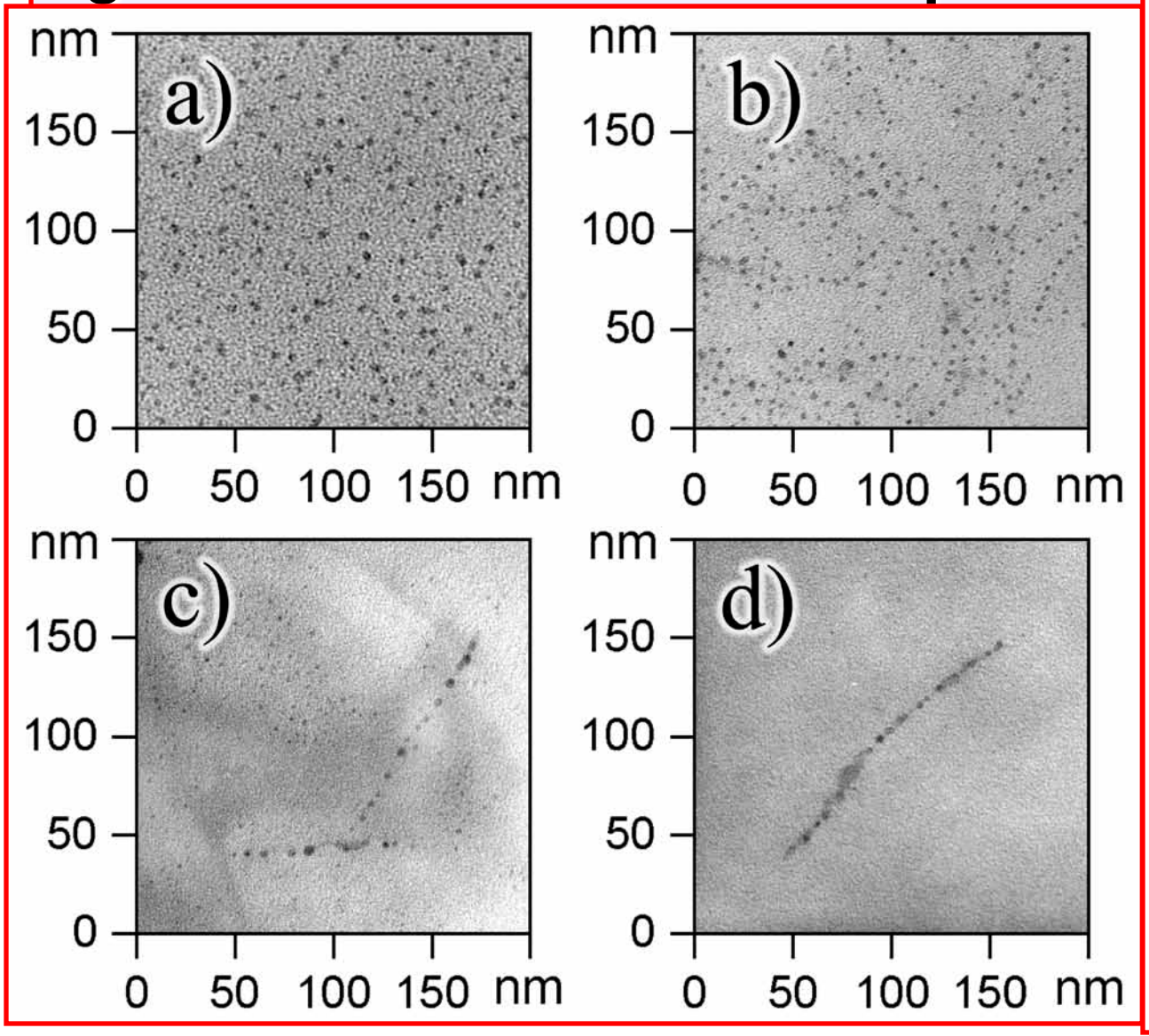

Image a): Iron oxide nanoparticles grown in ferrous arachidate 5-bilayer LB film (incubation time in the sodium borohydride solution (10^{-4} M) 1 hour).

Image b): Iron oxide nanoparticles grown in DNA/Fe^{3+}/PVP-16 complex LB film (incubation time in the sodium borohydride solution (10^{-4} M) 1 hour). DNA/Fe^{3+}/PVP-16 complex film was formed via the incubation of DNA/PVP-16 LB film in the $FeCl_3$ solution (2´ 10^{-4} M, pH = 2.5) for 1 hour.

Image c): Iron oxide nanowire grown in DNA/Fe^{3+}/PVP-16 complex LB film (incubation time in the sodium borohydride solution (10^{-4} M) 2 hours).

Image d): CdS nanowire grown in DNA/Cd^{2+}/PVP-16 complex LB film via the incubation of corresponding precursor film contatining Cd^{2+} cations (DNA/Cd^{2+}/PVP-16 complex film) in the H_2S atmosphere for 2 hours. DNA/Cd^{2+}/PVP-16 complex film was formed via the incubation of DNA/PVP-16 LB film in the $CdCl_2$ solution (2´ 10^{-4} M, pH = 6.0) for 1 hour.

TEM micrographs showing self-organized DNA complexes with cationic CdSe Q-rods

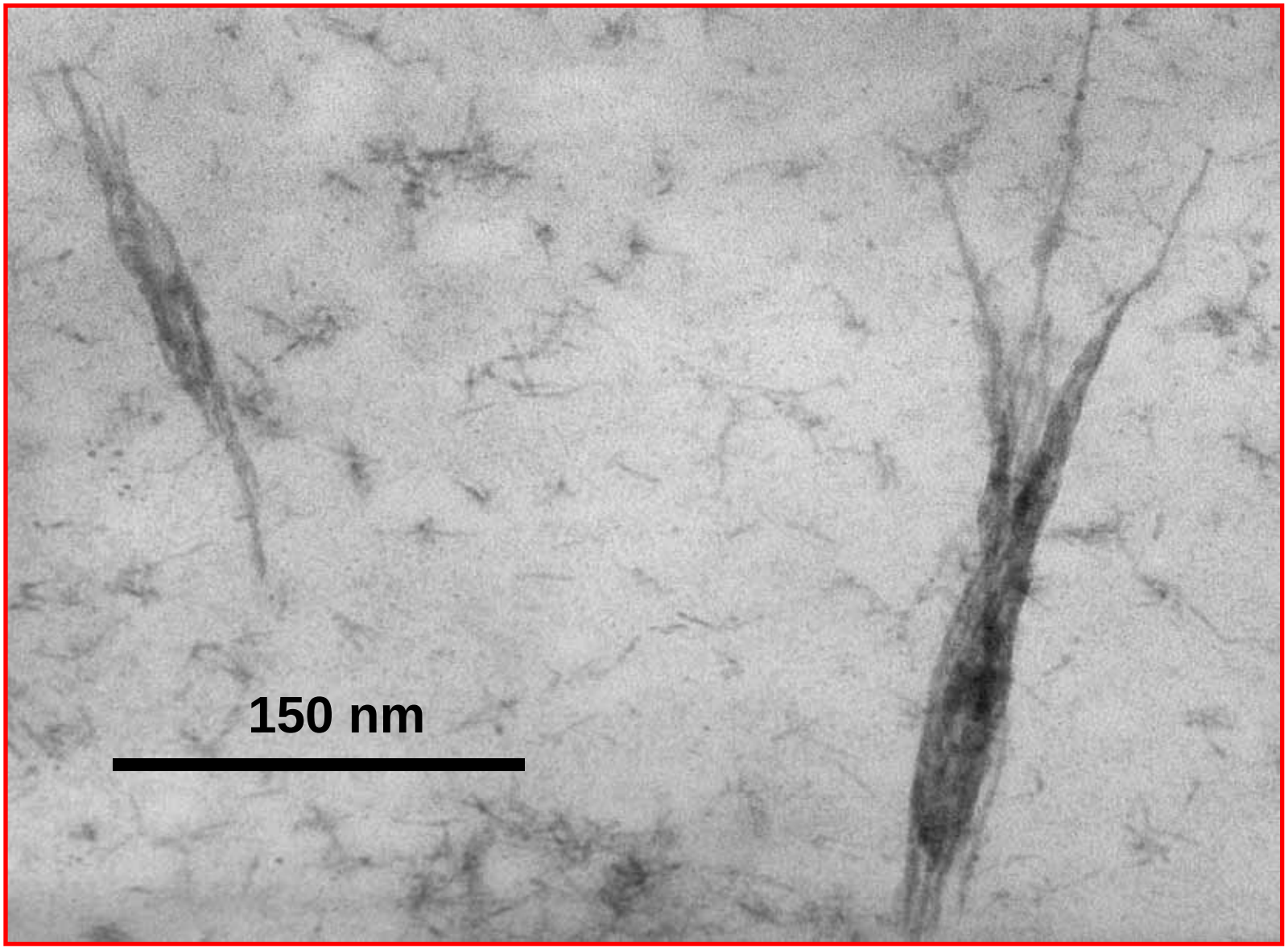

Transmission electron micrographs showing self-organized DNA/CdSe Q-rods complexes

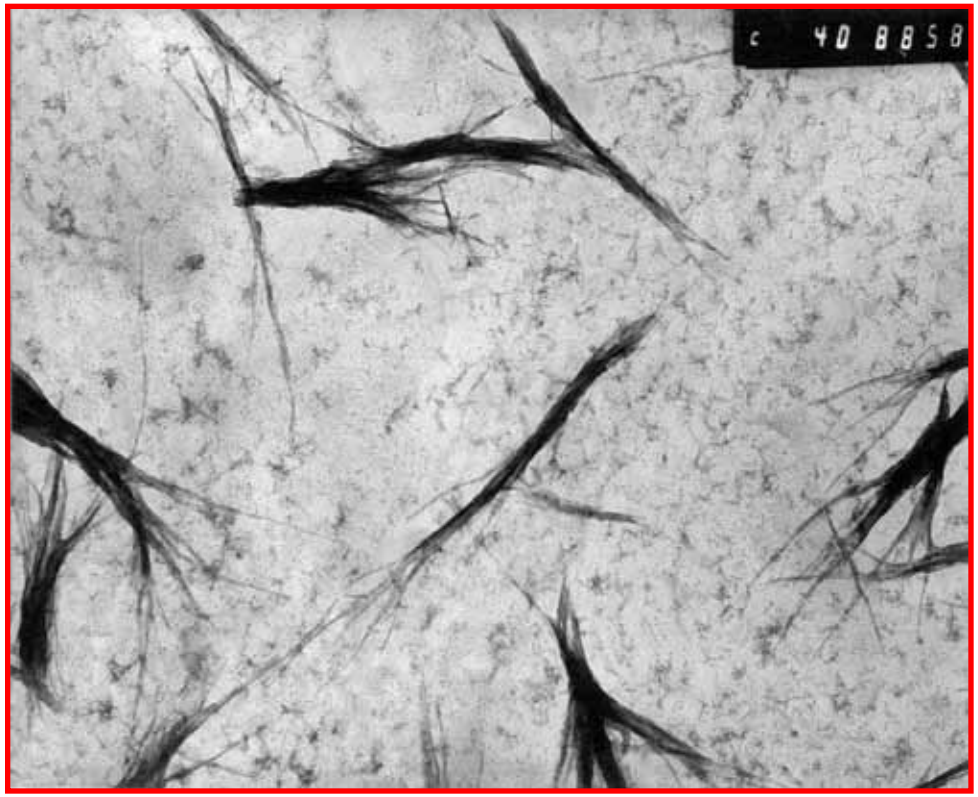

500 nm

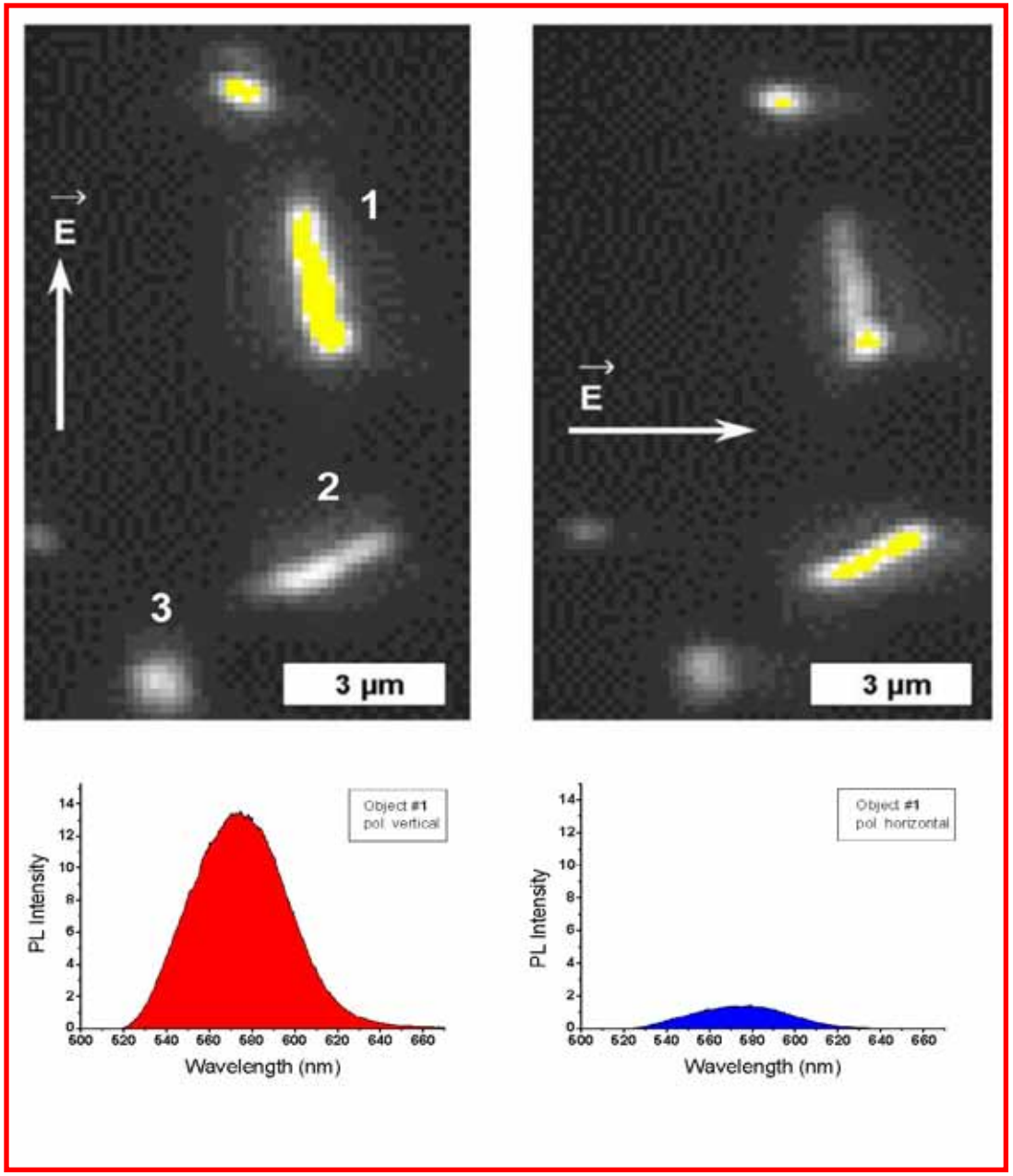

M. Artemiev et.al., J. Am. Chem. Soc., 2004, Vol.126, p.10594-10597.

Room temperature polarized micro-photoluminescence images of DNA/CdSe nanorods complexes

The images were obtained using optical setup including cw Ar-ion laser as the excitation source (λ=488 nm, 50 mW), objective Zeiss Achromate, ´ 20, CCD video camera and high resolution imaging monochrometer equipped wiht CCD camera. The collected light was filtered with 2 mm orange filter placed just after the objective in order to completely remove scattered laser light. The rotating linear polarization filter was placed behind the orange filter. The polarization is vertical on the left image and horizontal on the right one. Both images are represented in false-color scale with PL intensities increased from black through white to yellow. At the bottom corresponding room temperature PL spectra of the object 1 confirm strong polarization of emission along the filament.

Transmission electron micrographs of organized DNA complexes with magnetite nanoparticles

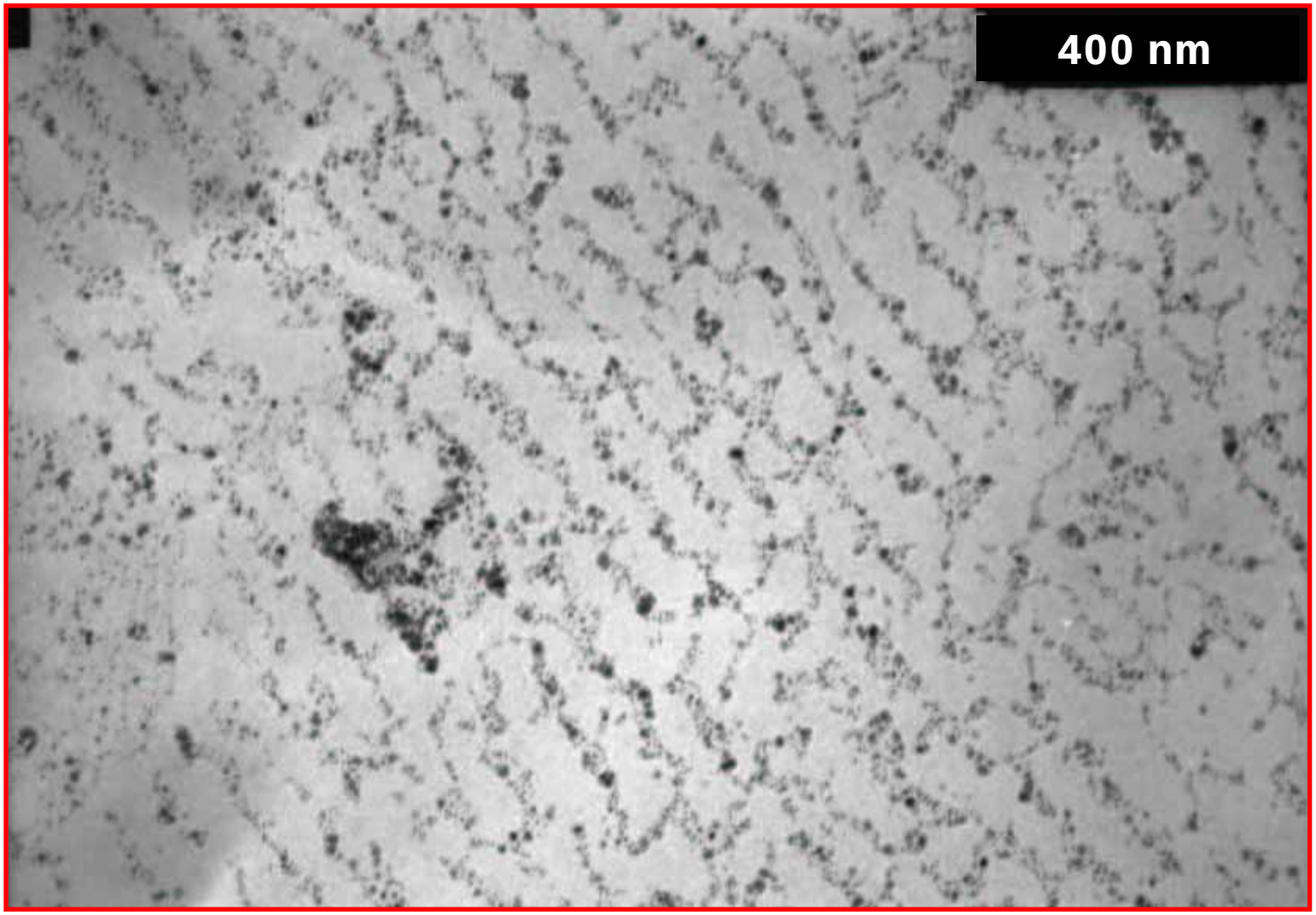

DNA/PVP-20 net-like complex deposited on solid substrate was incubated in aqueous solution of cationic Fe_3O_4 nanoparticles (pH=3).

Transmission electron micrographs of organized DNA complexes with magnetite nanoparticles

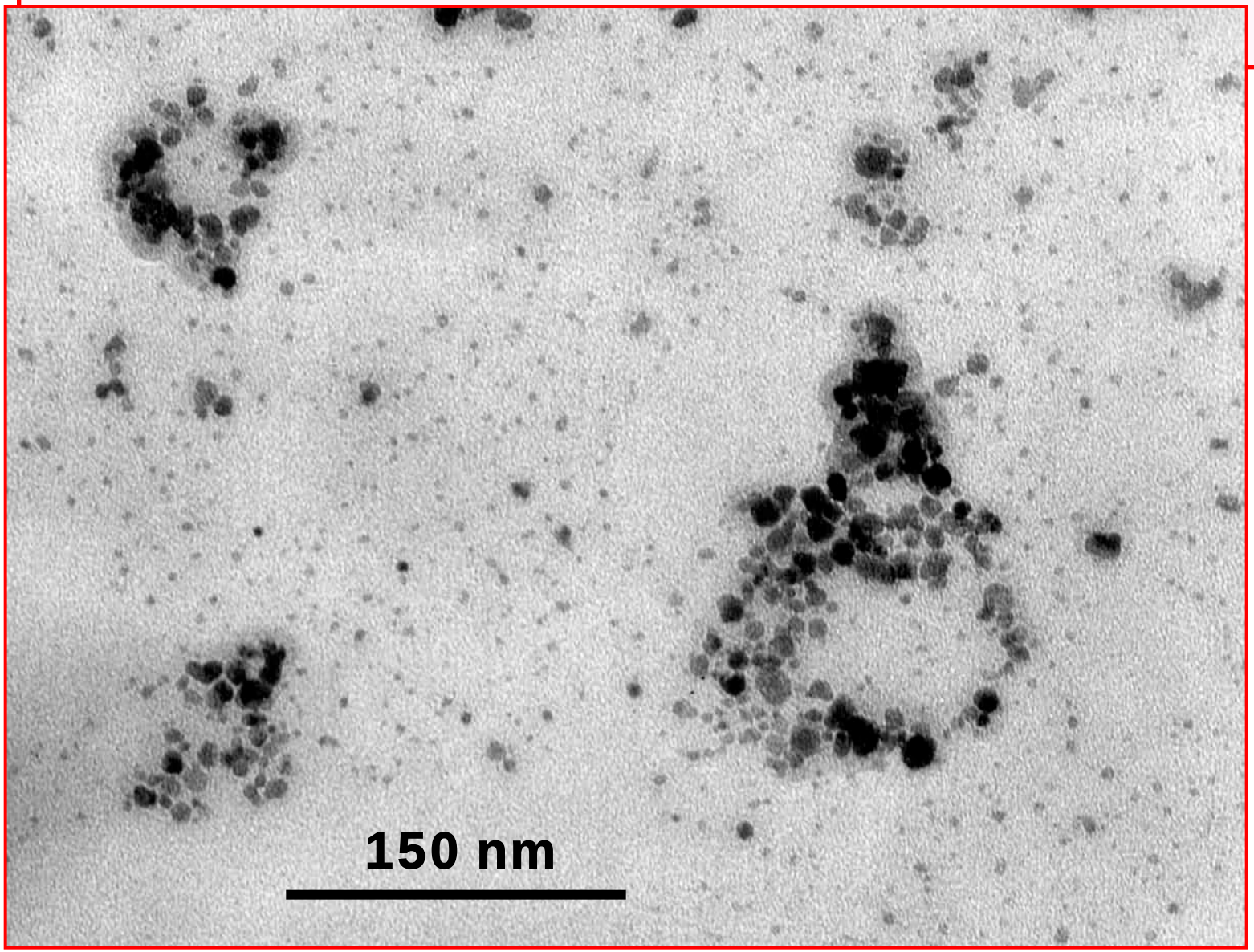

DNA/PVP-20 toroidal complex deposited on solid substrate was incubated in aqueous solution of cationic Fe_3O_4 nanoparticles (pH=3).

DNA complexes with magnetic Fe_3O_4 nanoparticles in a bulk aqueous phase

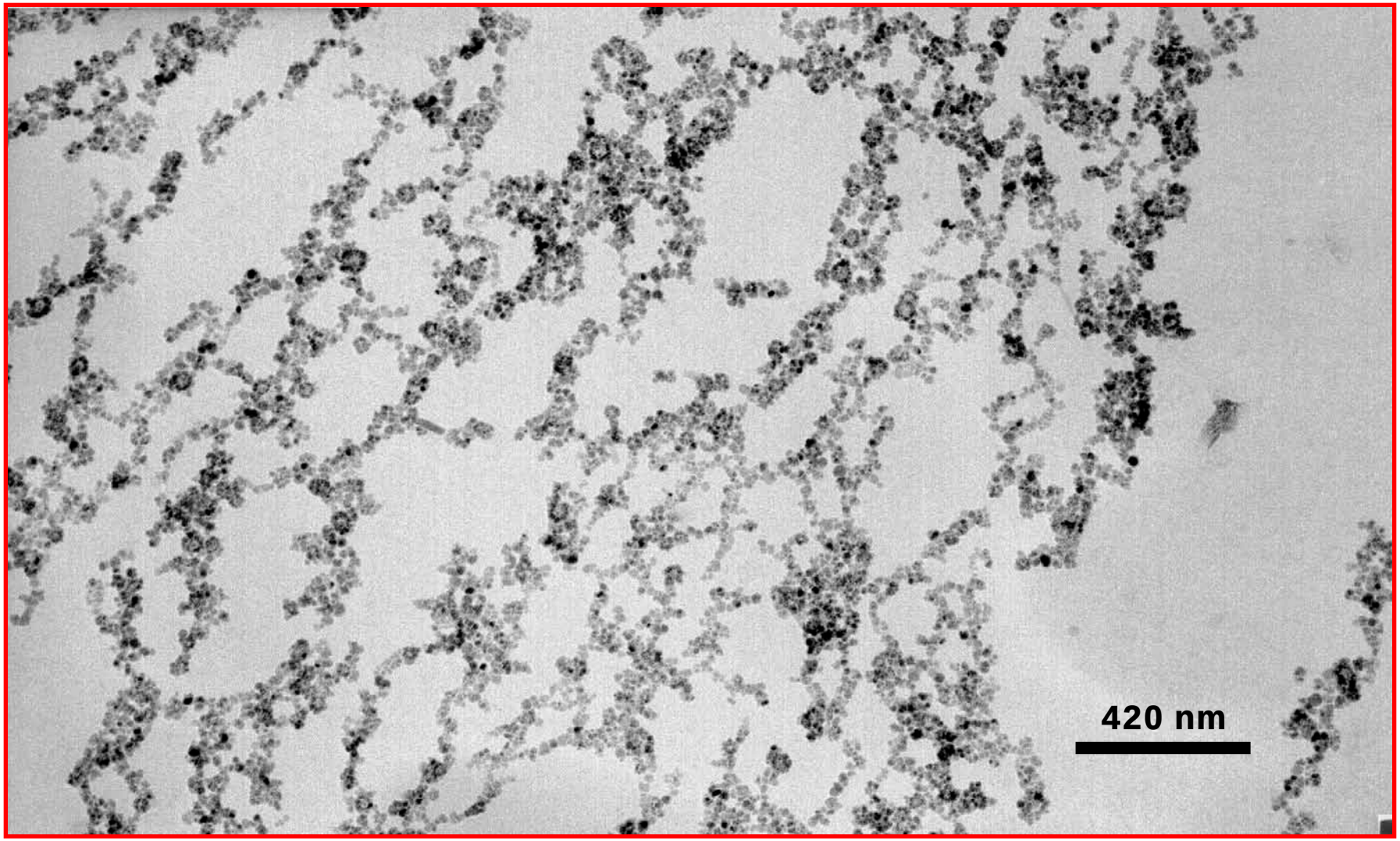

EPR spectra of Fe_3O_4 nanoparticles (~ 5 nm diameter) in aqueous phase

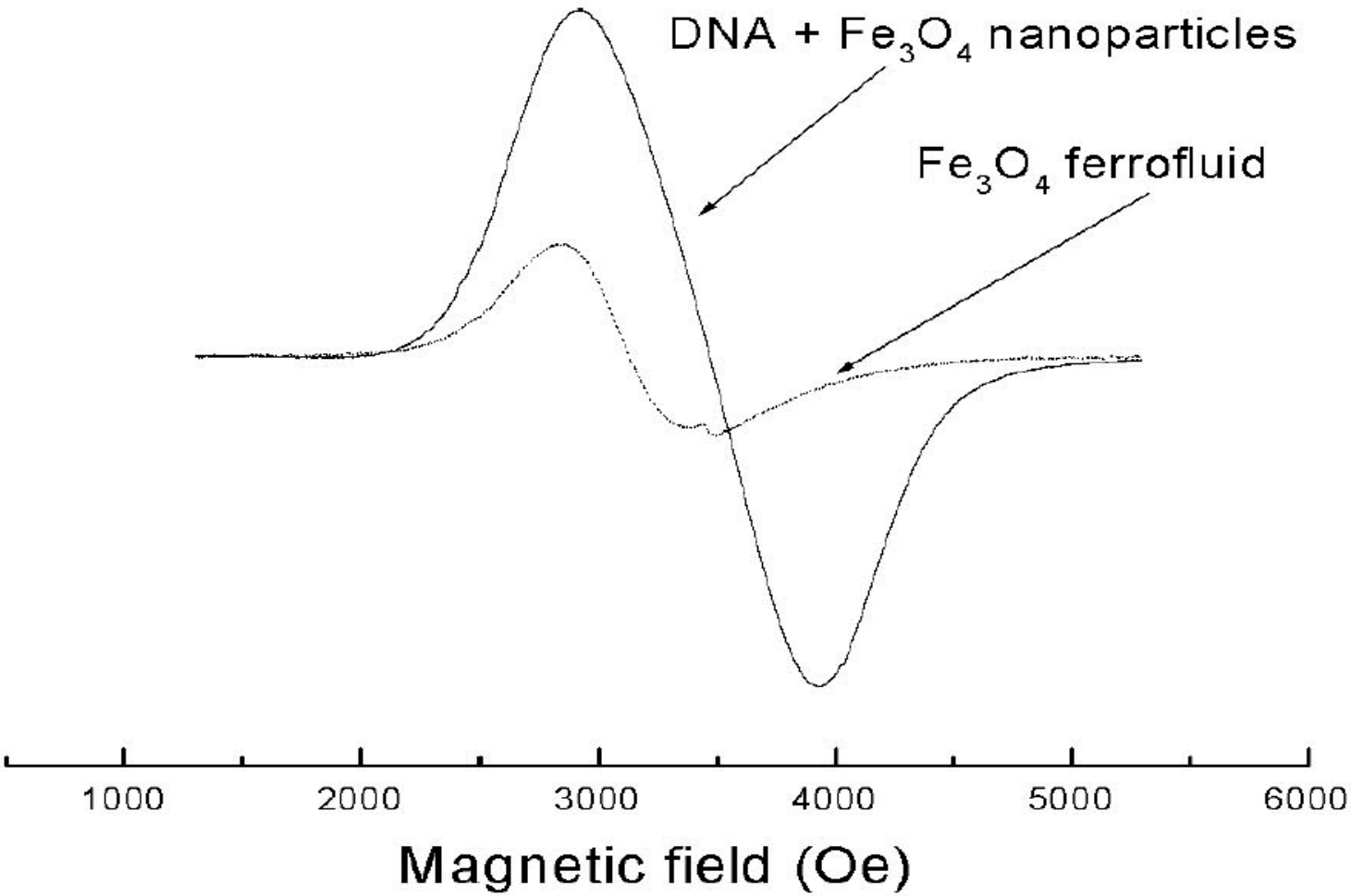

4. Investigation of Iron oxide nanoparticles formation in immobilized DNA complexes in presence of only biogenic reagents

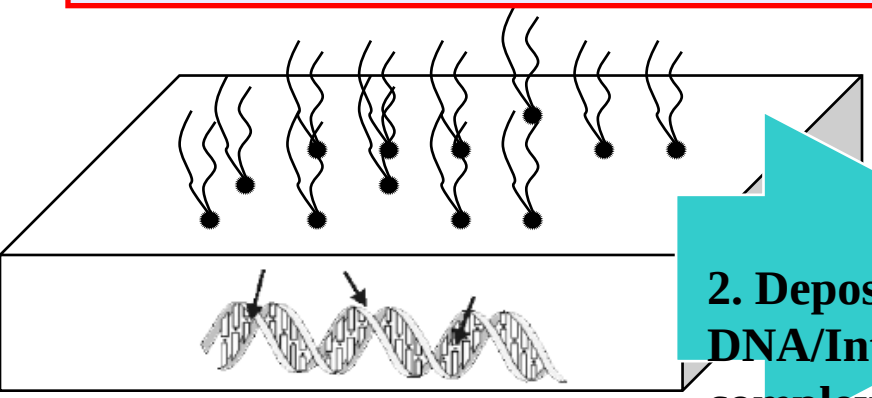

1. DNA binding with intercalator Langmuir monolayer

2. Deposition of DNA/Intercalator complex to solid substrate

3. Incubation in Ferritin suspension

4. Washing in water

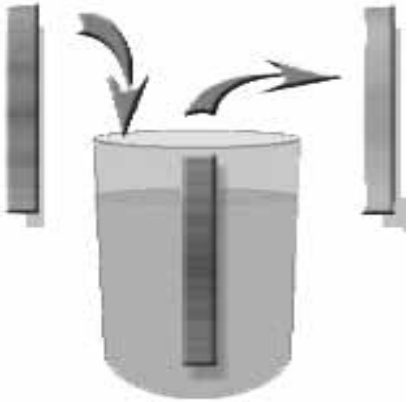

5. Incubation in reductant solution (ascorbic acid or $NaBH_4$).

6. Washing in water

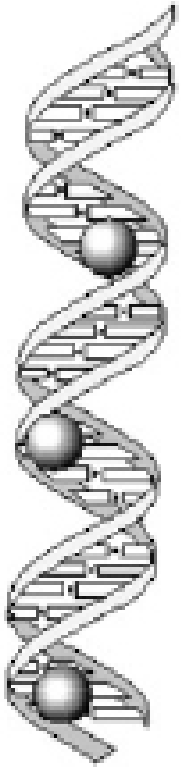

DNA was immobilized via binding with Langmuir monolayer of amphiphilic intercalating dye N,N'-Dioctadecyloxacarbocyanine -4-toluenesulfonate

Ferritin

Synthesis of iron oxide nanoparticles with ferritin as a source of iron

Ferritin is known as a spherical protein complex composed of protein shell and an inorganic iron-containing core in the form of a hydrous ferric oxide. The inner inorganic core of the protein complex is usually 5-8 nm in diameter and is able to incorporate about 4500 iron atoms in the form of paracrystalline iron oxyhydroxide.

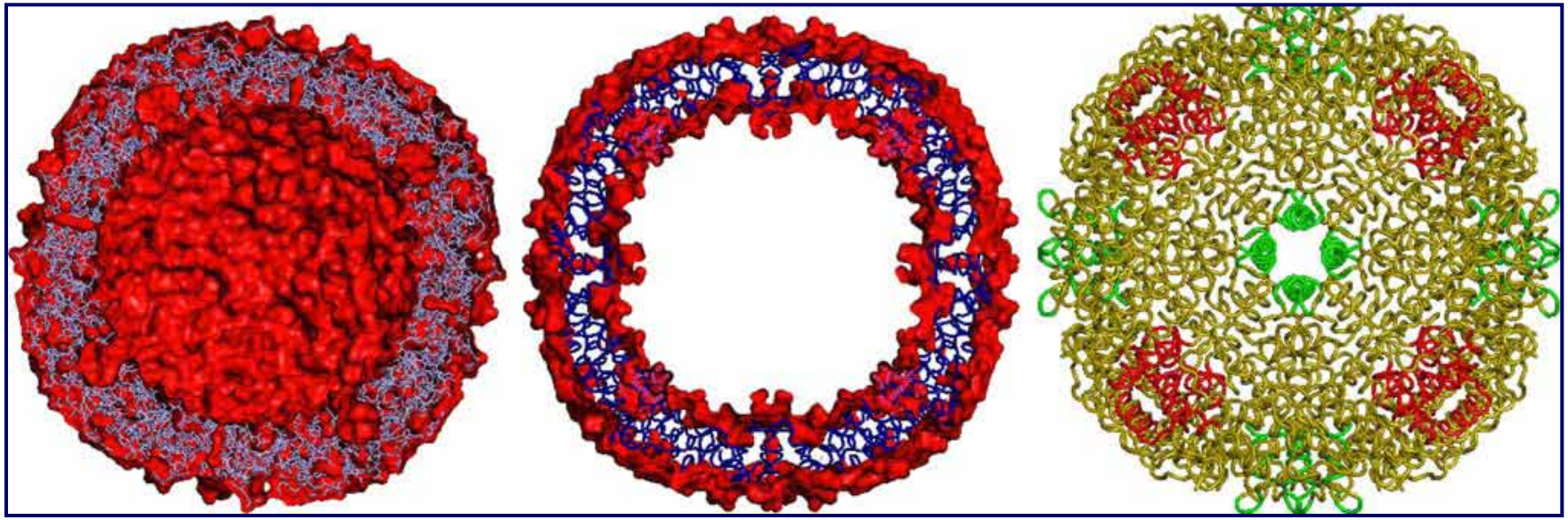

Maxi-ferritin structure. Left and middle: Cross sections showing large protein central cavity (left), the central slab of the protein cage (middle); right: ribbon diagram with the C3 pore shown in red; the C4 pore, absent in some ferritin protein crystals and very large in others, is shown in green.
From: E.C. Theil, M. Matzapetakis, X. Liu, Ferritins: iron/oxygen biominerals in protein nanocages, J. Biol. Inorg. Chem. (2006) 11:803–810.

Ferritin

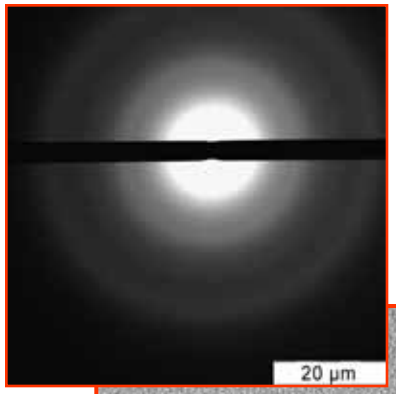

¬ selected area electron difractogramm

TEM micrographs

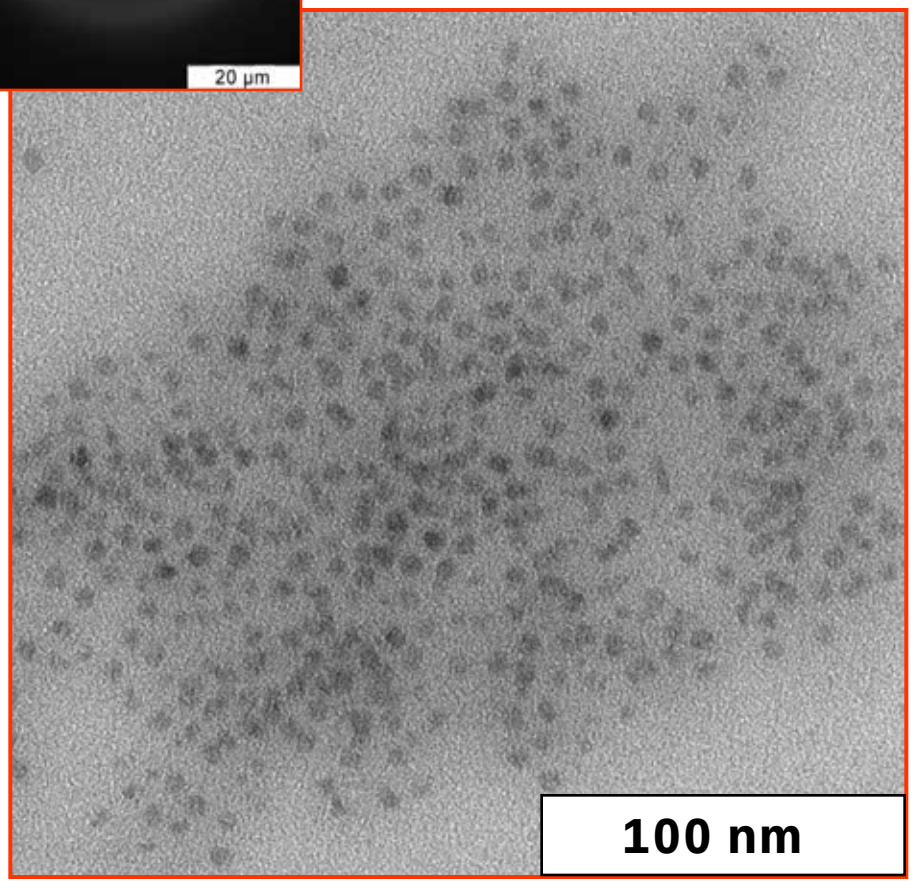

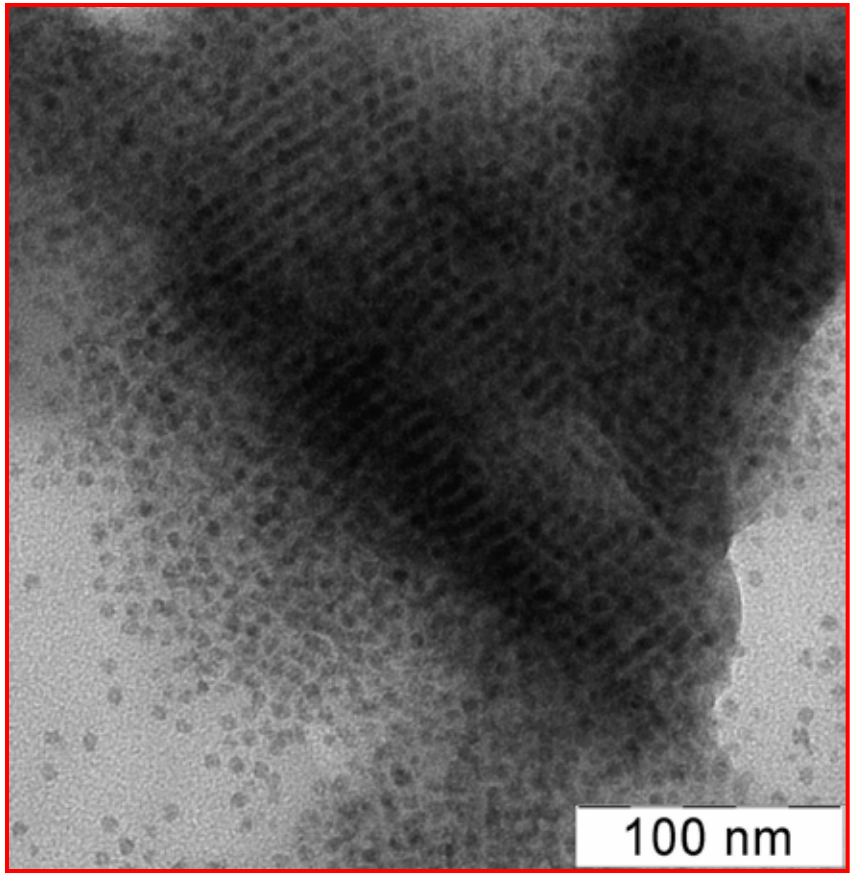

TEM image of deposited amphiphilic dye monolayer with bound DNA molecules

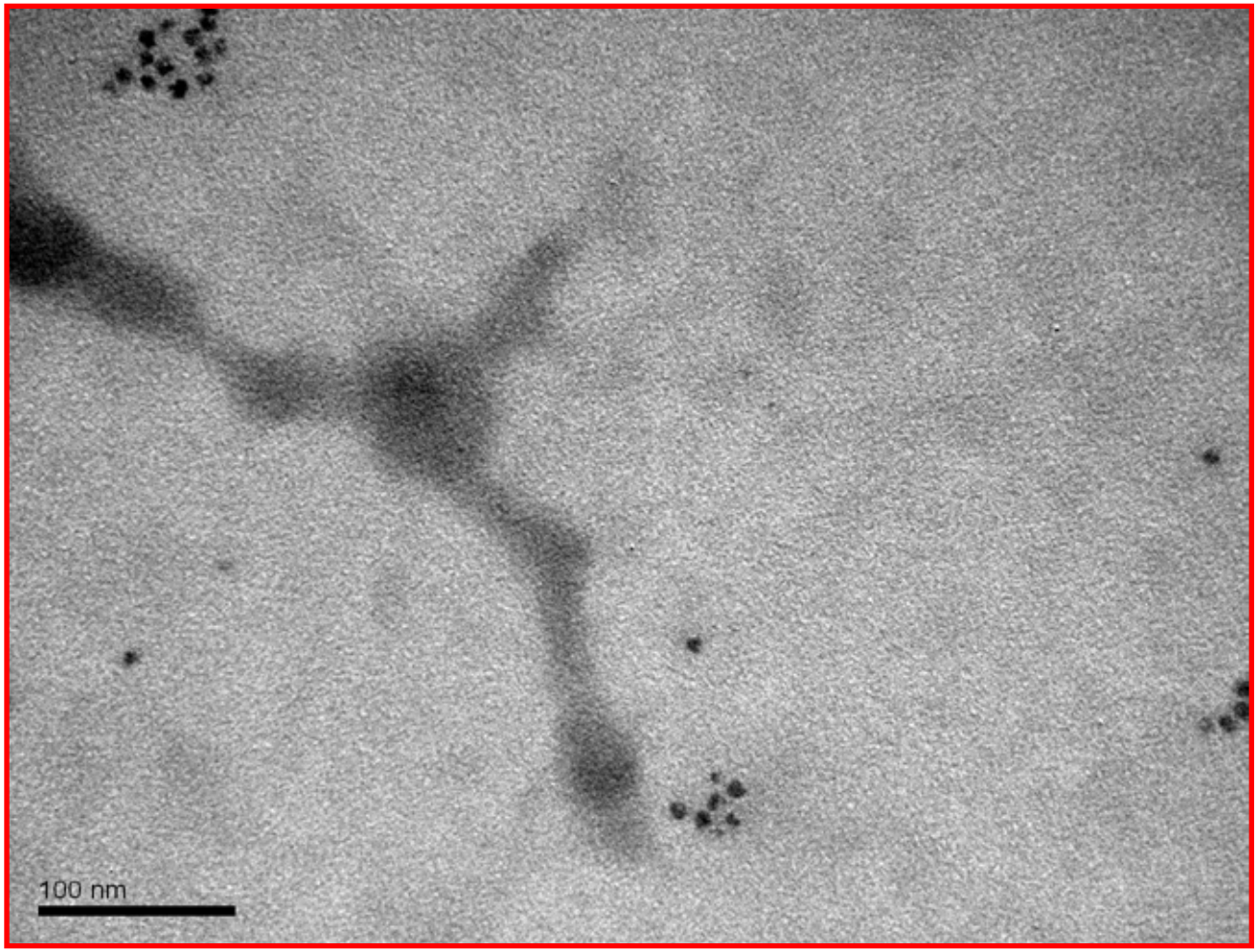

DNA was immobilized via binding with Langmuir monolayer of amphiphilic intercalating dye N,N'-Dioctadecyloxacarbo cyanine-4-toluenesulfonate followed by monolayer deposition onto TEM substrate.

Sample was incubated in ferritin suspension for 1 hour

TEM micrographs of iron oxide nanoparticles synthesized with ferritin as source of iron

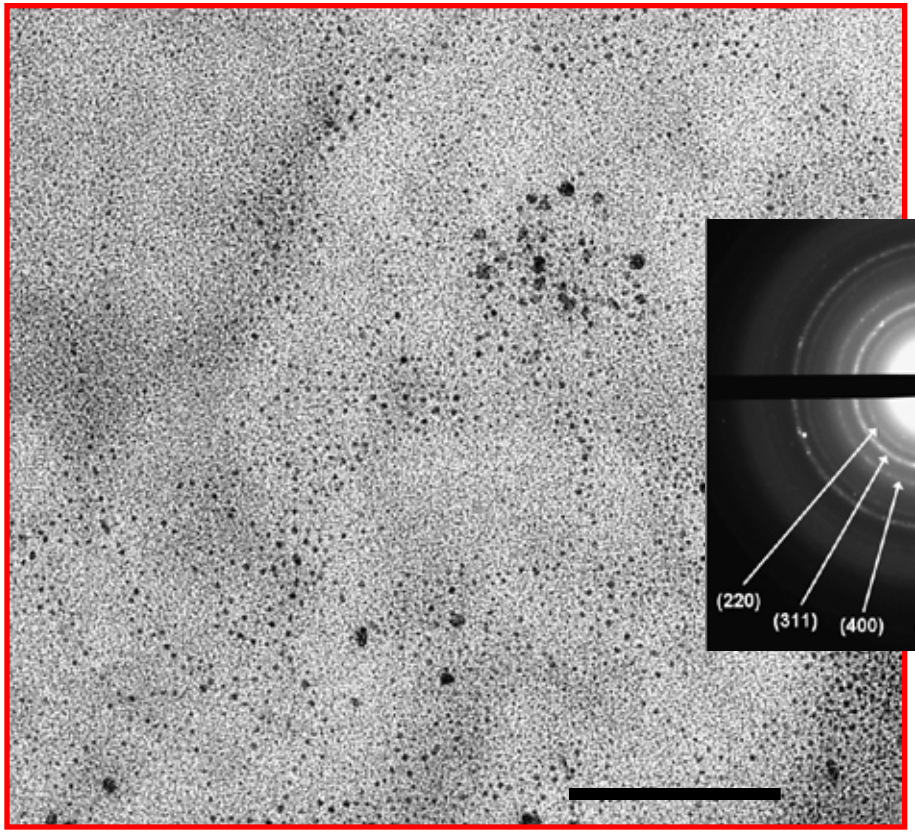

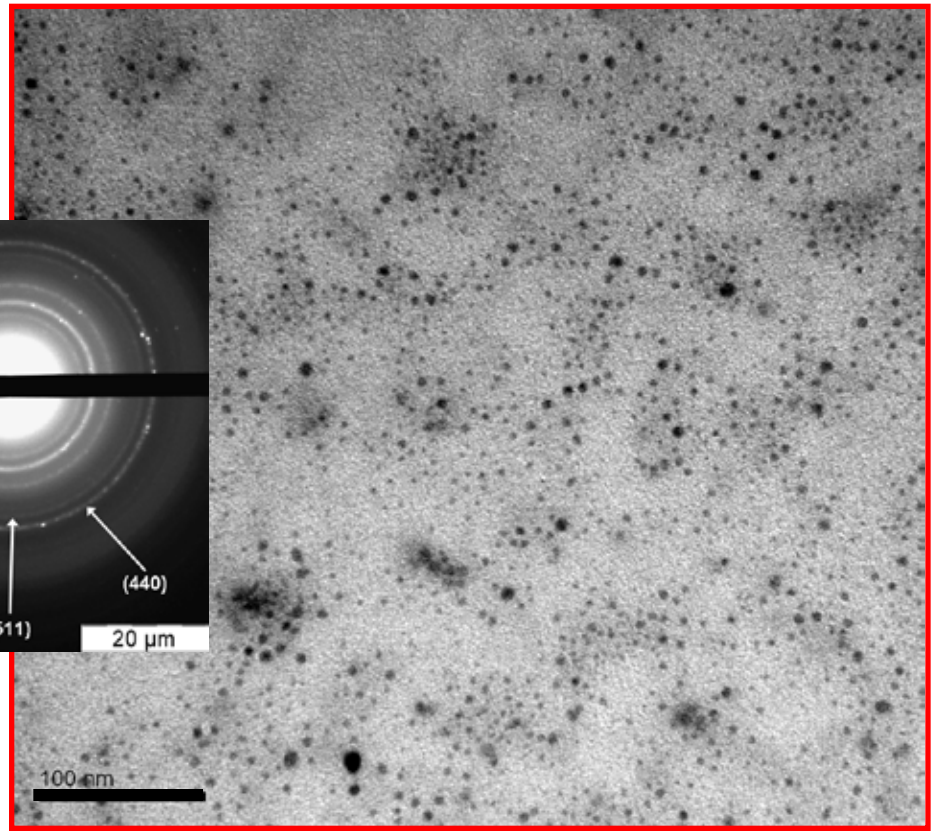

Iron oxide nanoparticles were synthesized via incubation of deposited amphiphilic dye monolayer with bound DNA molecules in ferritin suspension for 1 hour followed by incubation in ascorbic acid solution for 1 hour, pH=7.5. Bar size is 100 nm.

TEM micrigraph of iron oxide nanoparticles synthesized with ferritin as source of iron

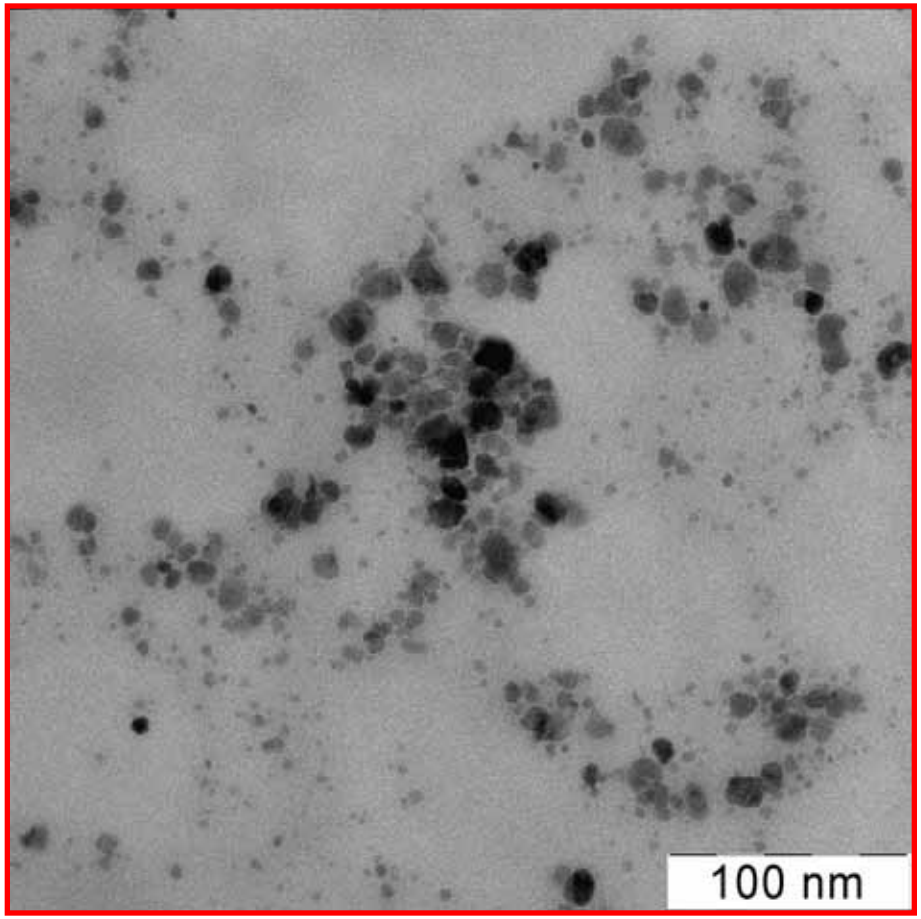

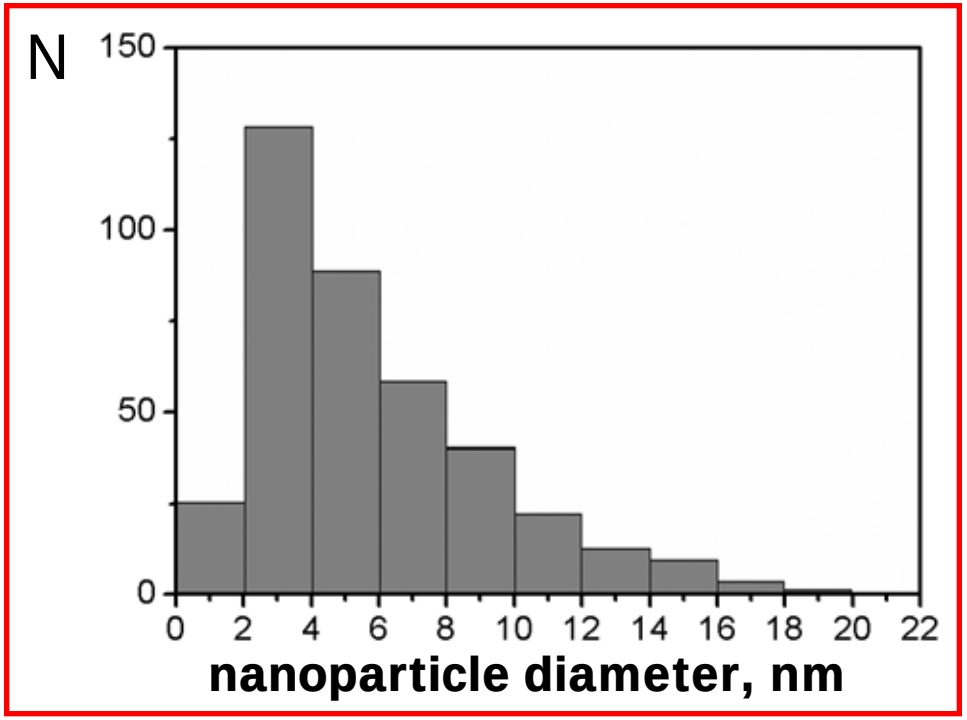

Size distribution hystogramm

Ferritin was used as an iron source, ascorbic acid was used as an reductant.
1 hour incubation, pH=7.5.

TEM micrigraph of iron oxide nanoparticles synthesized with ferritin as source of iron

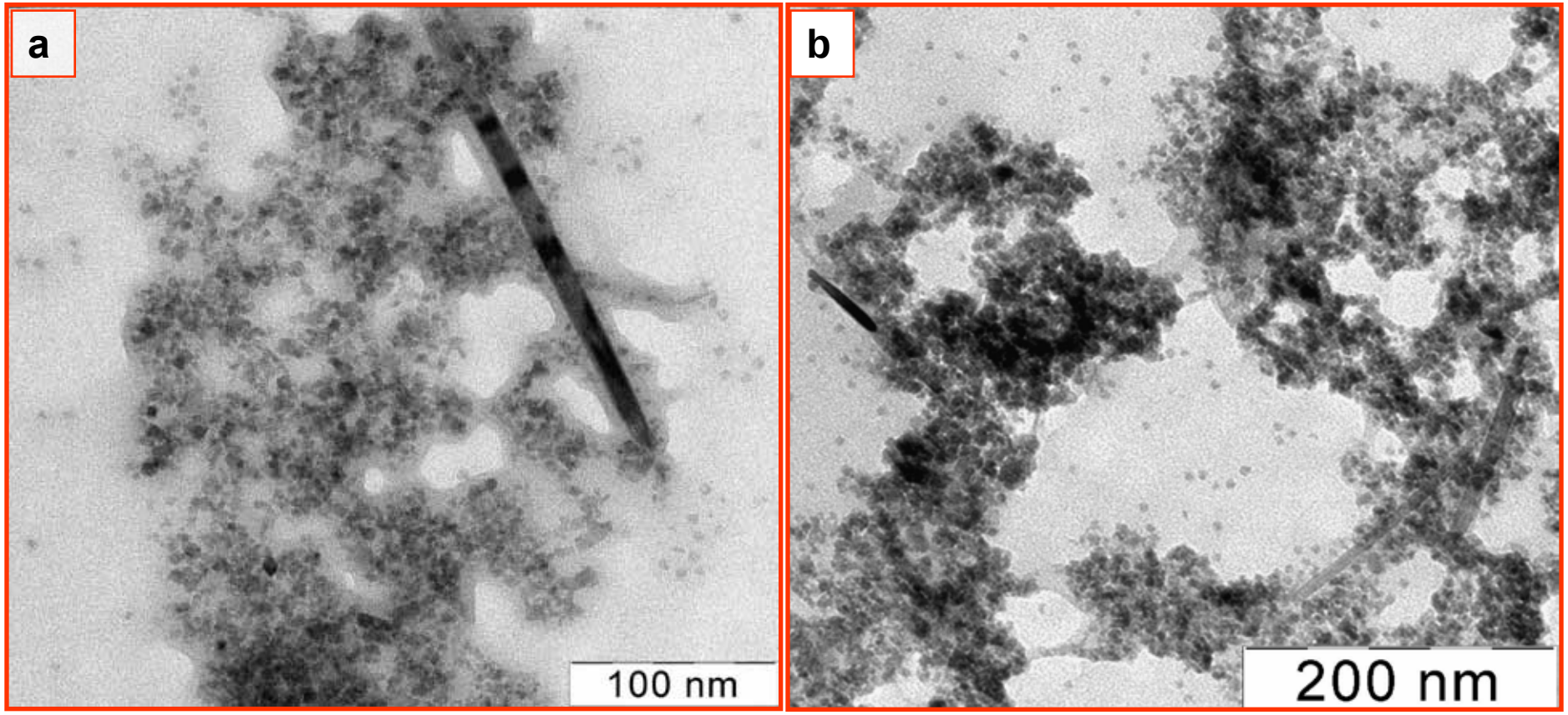

Ferritin was used as an iron source, incubation 24 hours
a): ascorbic acid was used as an reductant. b): $NaBH_4$ was used as a reductant.
pH=7.5.

5. Novel highly-organized nanofilm nanostructured materials and planar colloidal nanostructures representing the free-standing nanofilm in a liquid phase composed of chemically bonded colloid nano-components.

The approach to fabrication of that nanofilm material is based on controlled processes of self-assembly and self-organization of colloid nanoparticles via the formation of their complexes with polyfunctional ligands in a bulk liquid phase in the absence of any surfaces and interfaces.

РОССИЙСКАЯ ФЕДЕРАЦИЯ

ПАТЕНТ

НА ИЗОБРЕТЕНИЕ

№ 2336941

ТОНКОПЛЕНОЧНЫЙ МАТЕРИАЛ И СПОСОБ ПОЛУЧЕНИЯ ТОНКОПЛЕНОЧНОГО МАТЕРИАЛА

Патентообладатель(ли): *Хомутов Геннадий Борисович (RU), Кокшаров Юрий Алексеевич (RU)*

Автор(ы): *Кокшаров Юрий Алексеевич (RU), Хомутов Геннадий Борисович (RU), Кислов Владимир Владимирович (RU), Таранов Игорь Владимирович (RU)*

Заявка № 2006147123

Приоритет изобретения 29 декабря 2006 г.

Зарегистрировано в Государственном реестре изобретений Российской Федерации 27 октября 2008 г.

Срок действия патента истекает 29 декабря 2026 г.

Руководитель Федеральной службы по интеллектуальной собственности, патентам и товарным знакам

Б.П. Симонов

TEM micrographs of spermine complexes with magnetite nanoparticles (~10 nm diameter) formed in a bulk aqueous phase

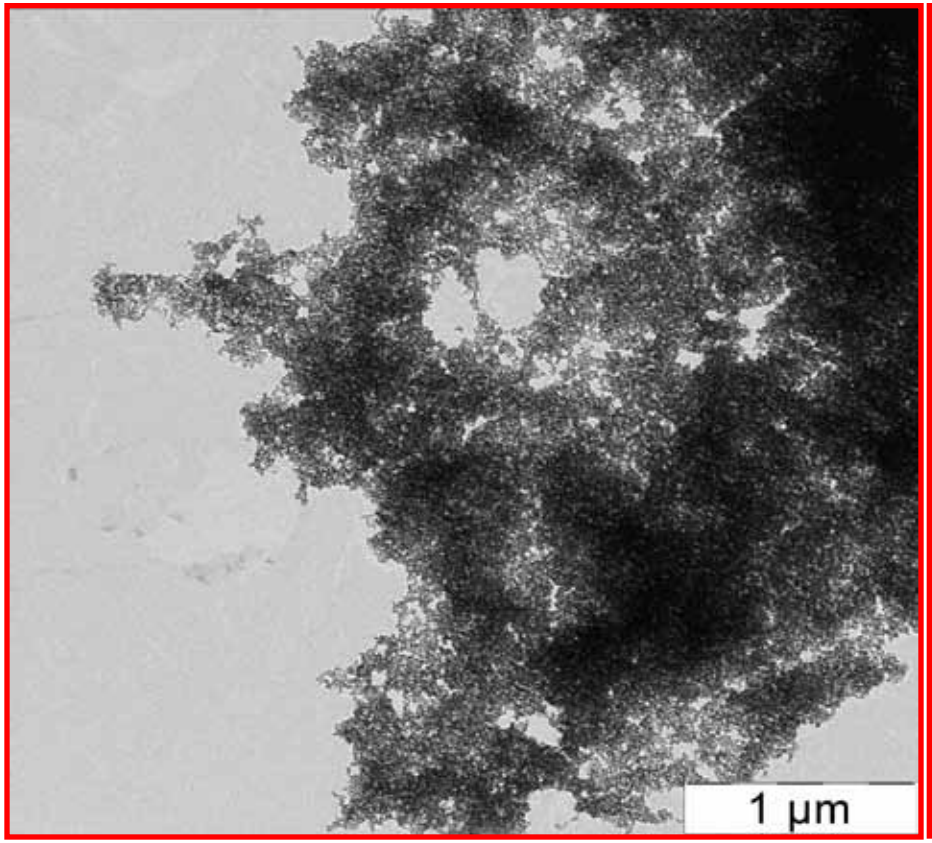

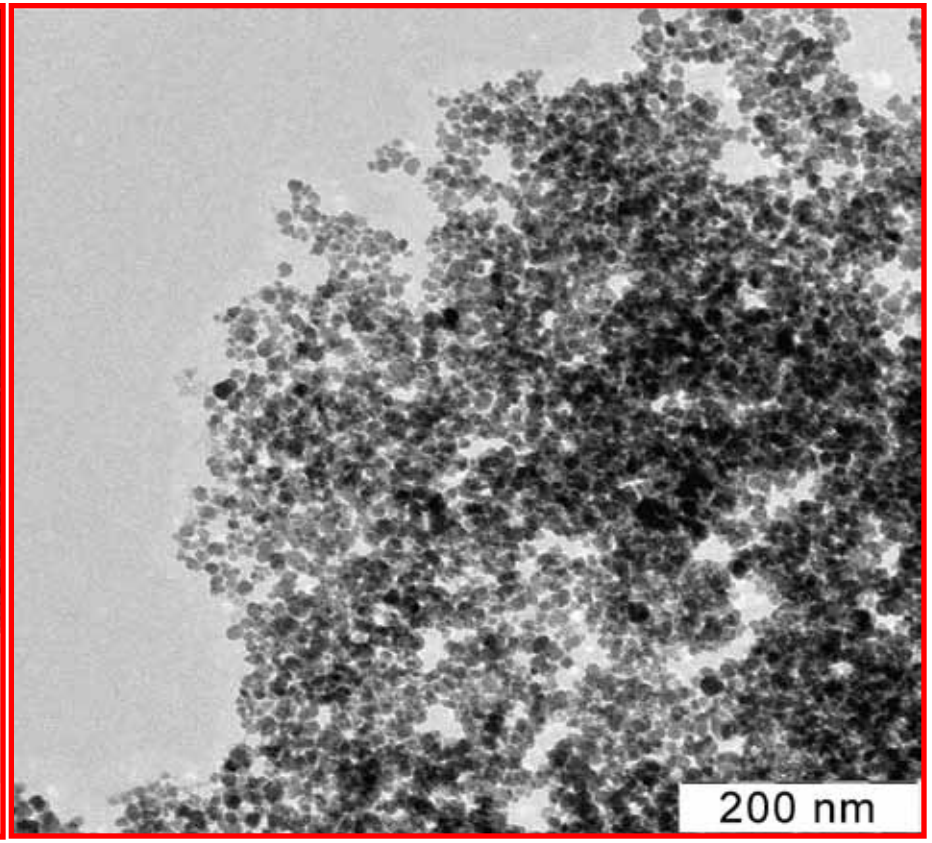

Spermine complexes with Fe_3O_4 nanoparticles at (pH~5.5).

TEM micrographs of self-assembled nanofilm material

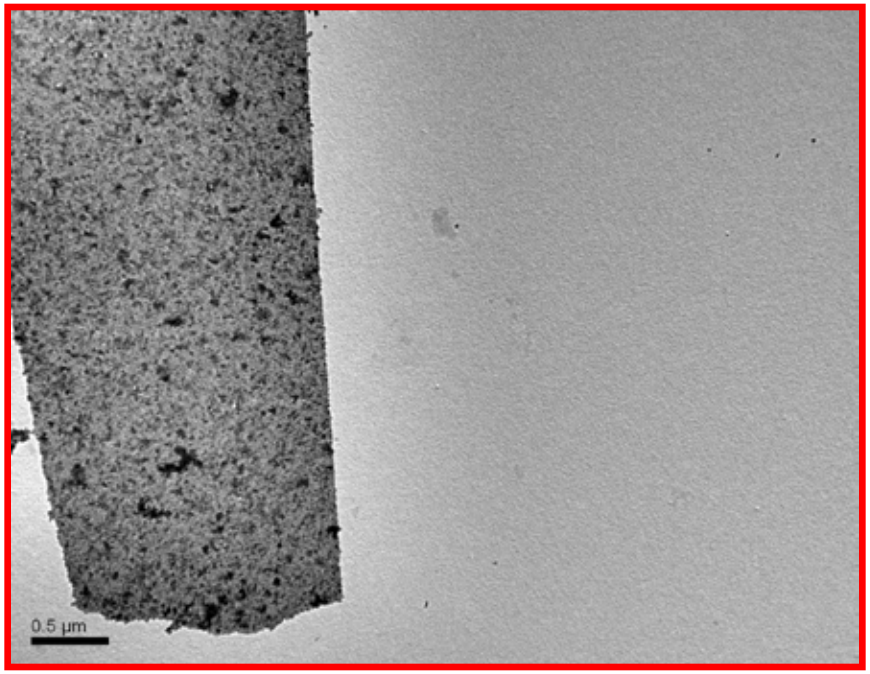

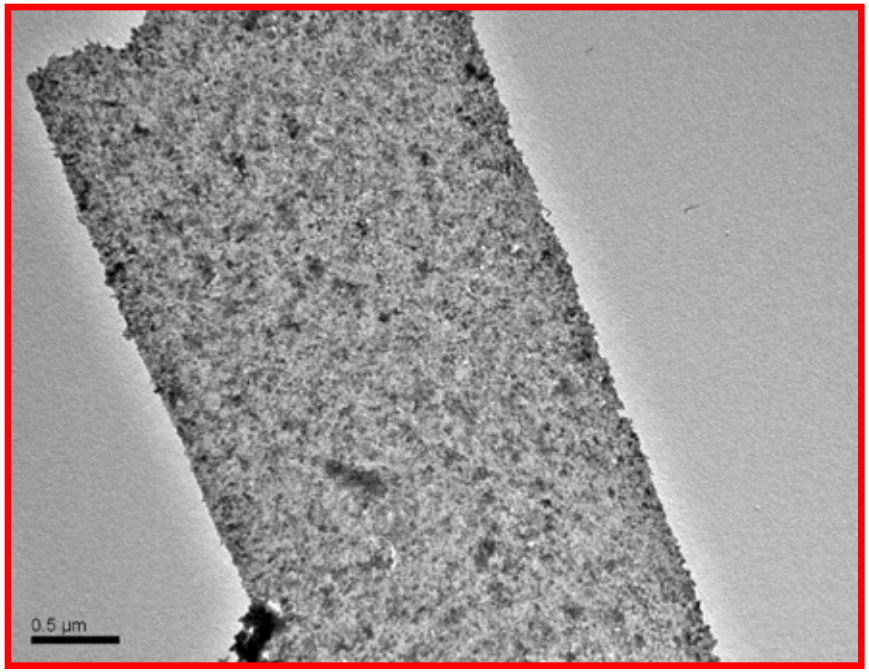

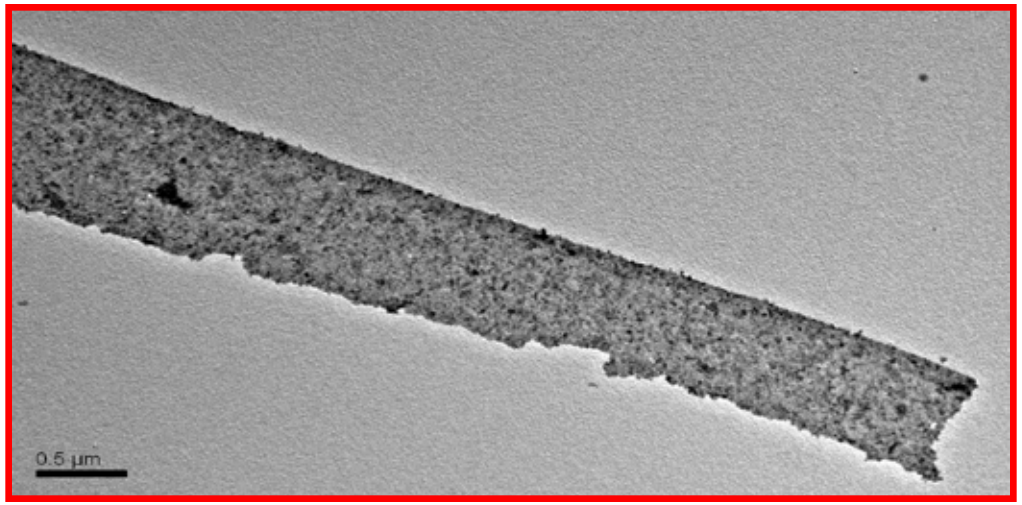

TEM micrographs of self-assembled nanofilm material

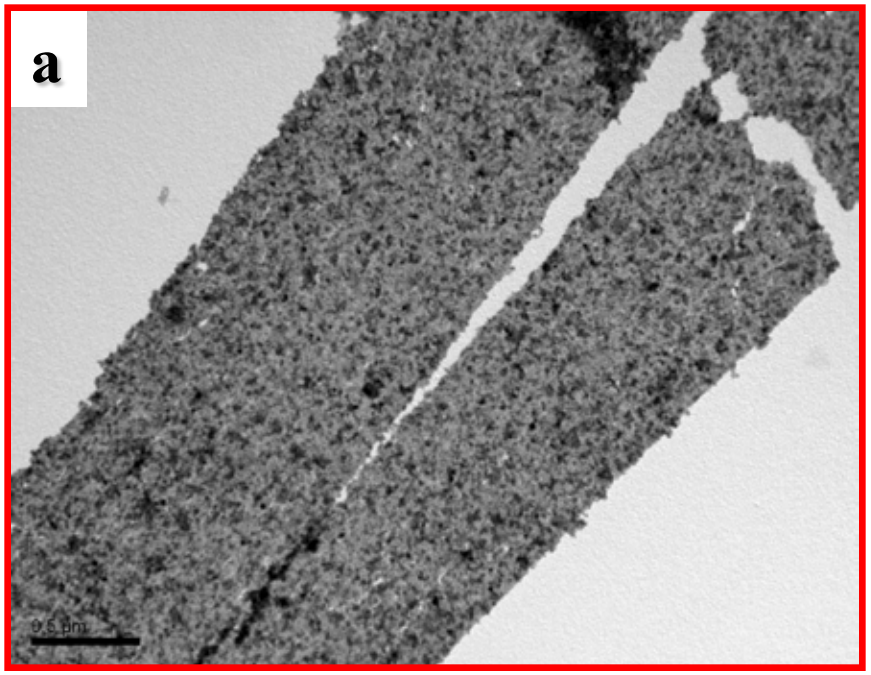

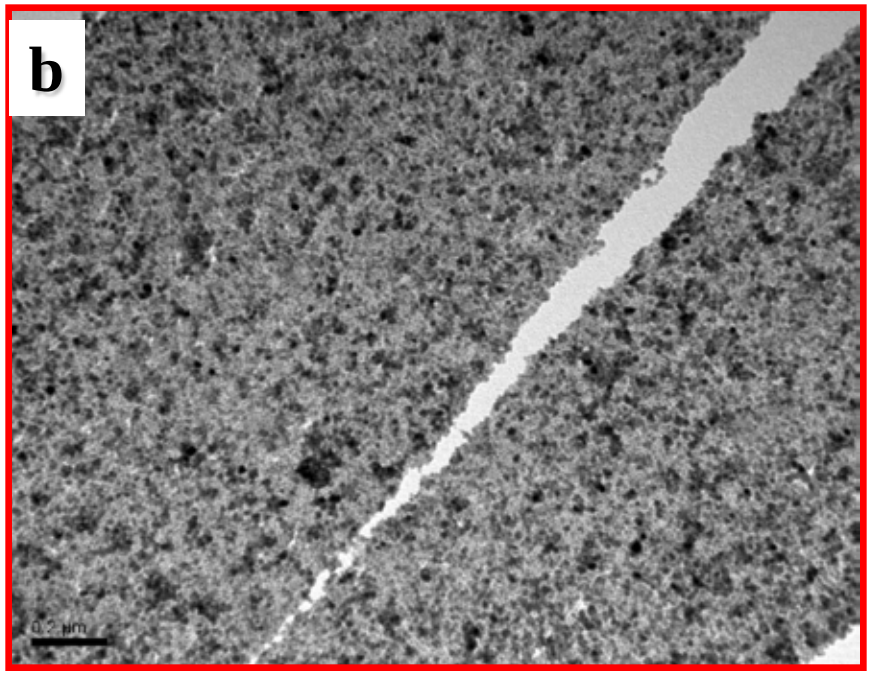

На рисунке представлены характерные изображения, на которых видно образование разрыва тонкопленочной структуры с образованием ровных прямолинейных границ. Образцы получены путем высушивания капли суспензии, содержащей полученные свободные тонкопленочные структуры микронных размеров, на поверхности стандартной подложки для просвечивающей электронной микроскопии (медная сетка, покрытая слоем полимера и углерода). Размер черной масштабной метки: (а) - 0.5 мкм., (б) - 0.2 мкм.

AFM image of of self-assembled nanofilm material deposited on mica surface

a

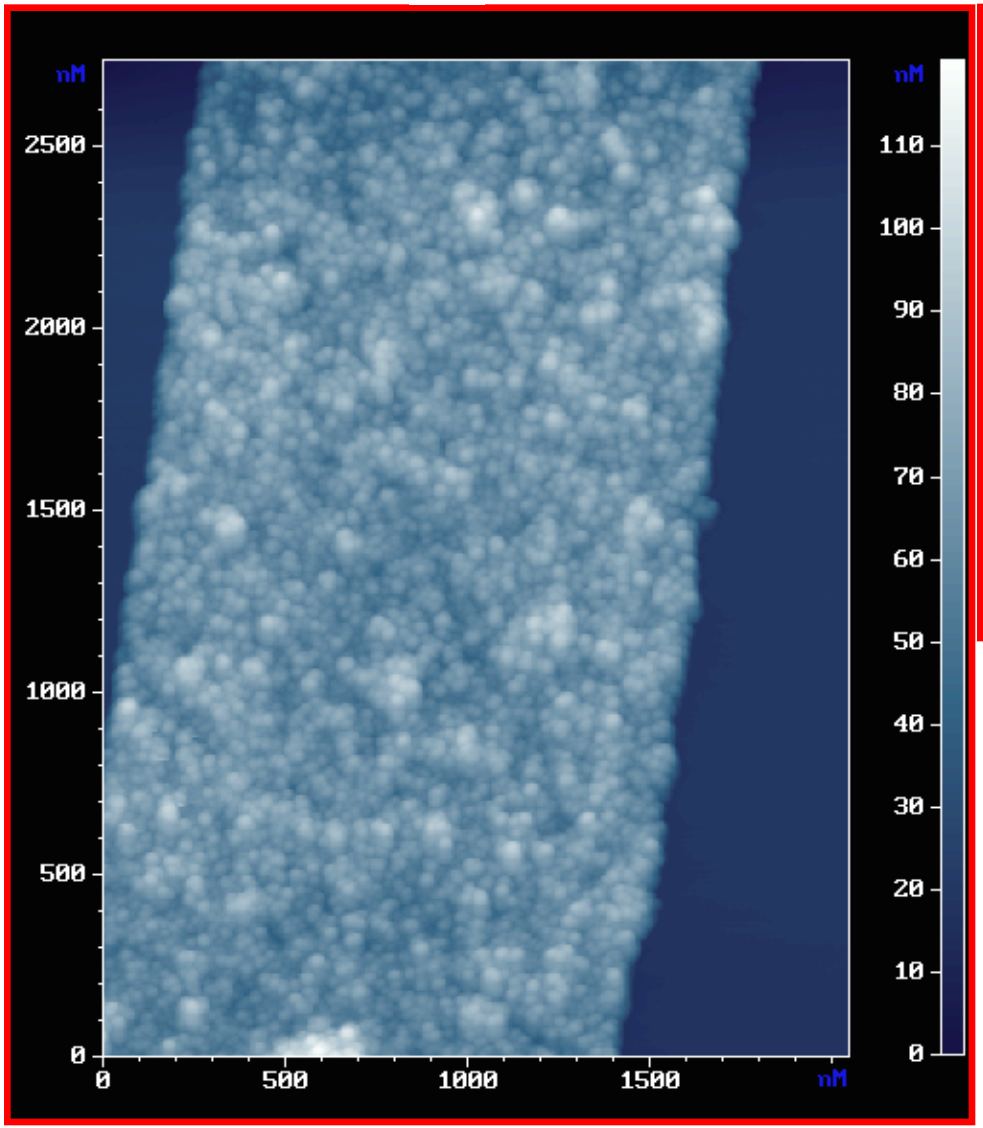

b

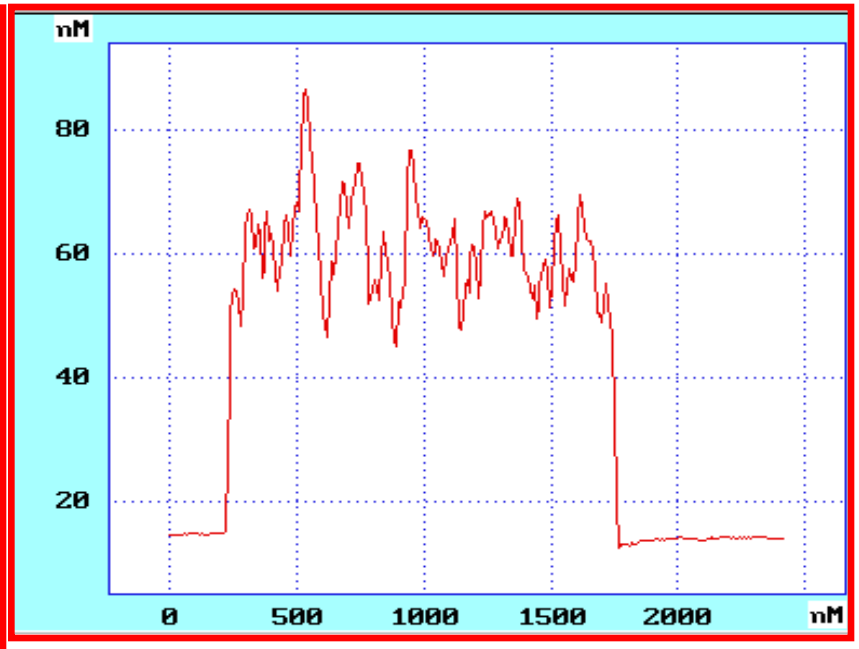

a): Topographyc image

b): Vertical cross-section profile

TEM micrographs of self-assembled nanofilm material

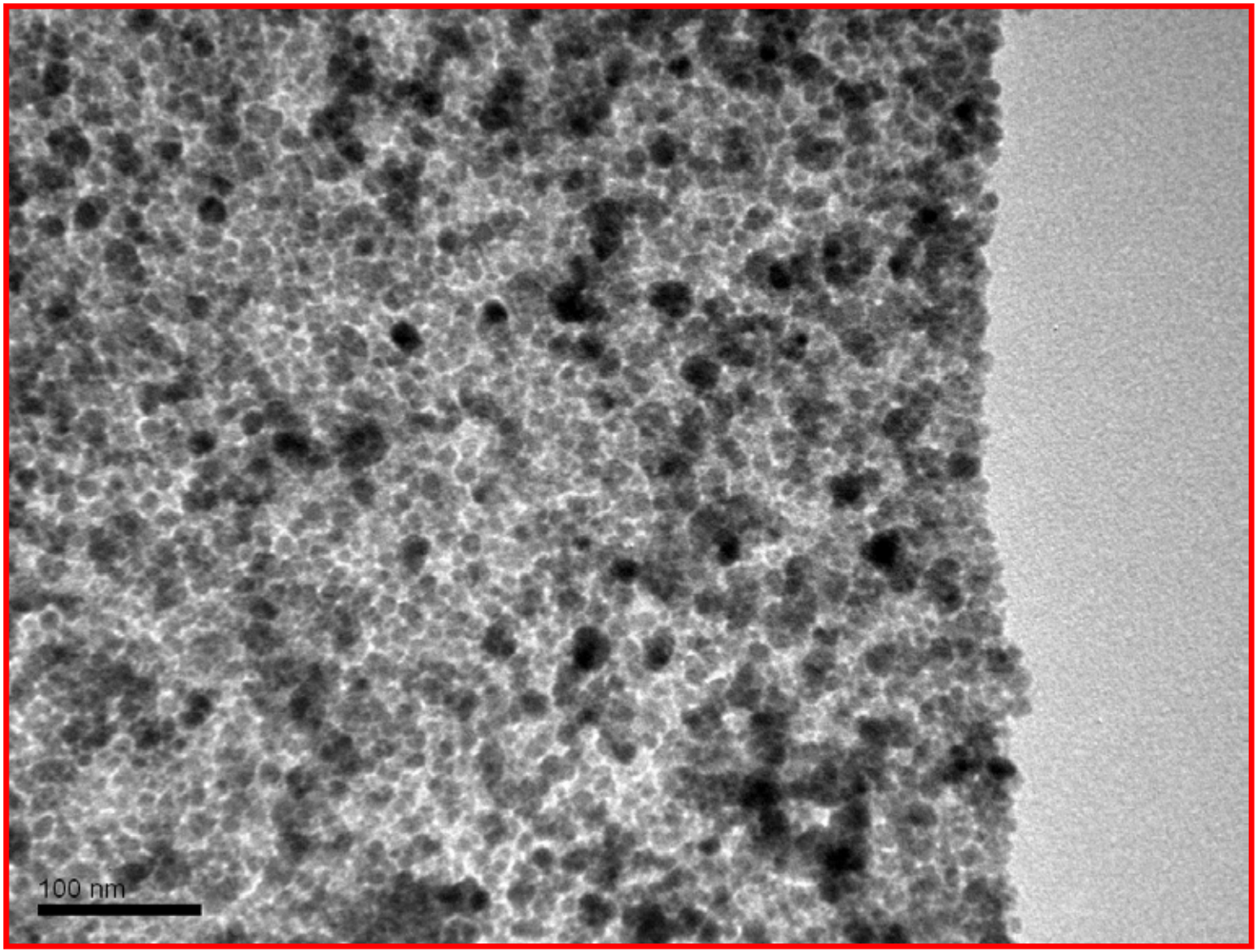

TEM micrographs of self-assembled nanofilm material

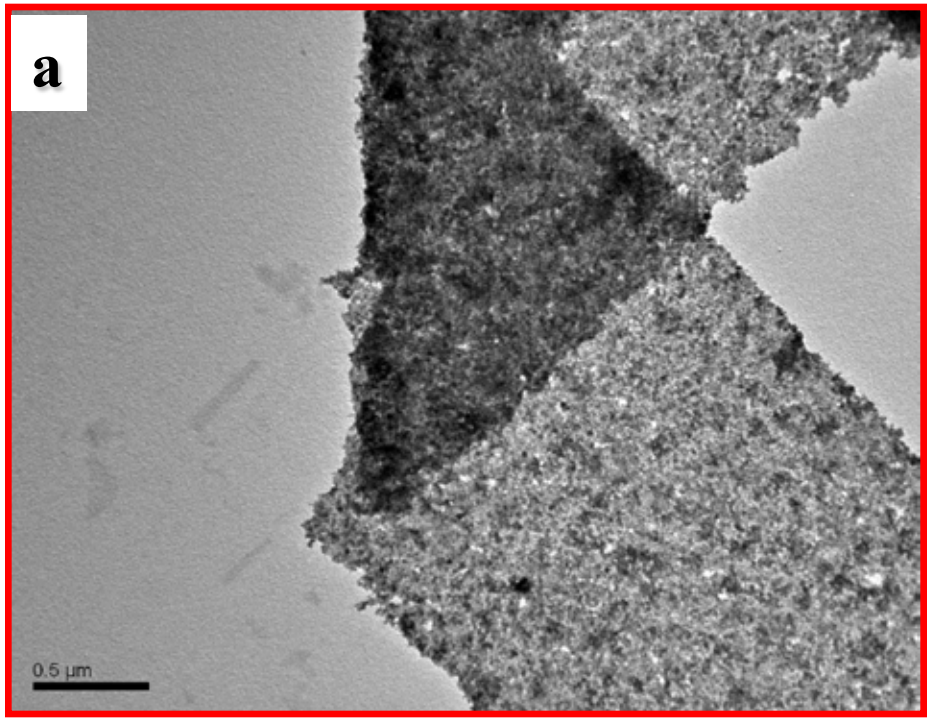

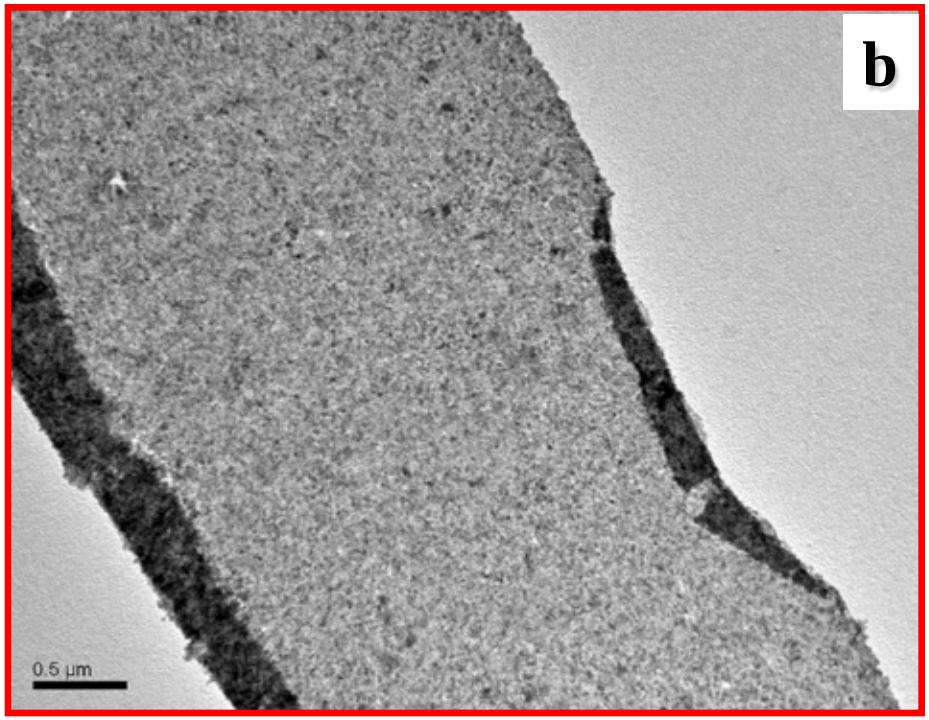

AFM image of of self-assembled nanofilm material deposited on mica surface

a

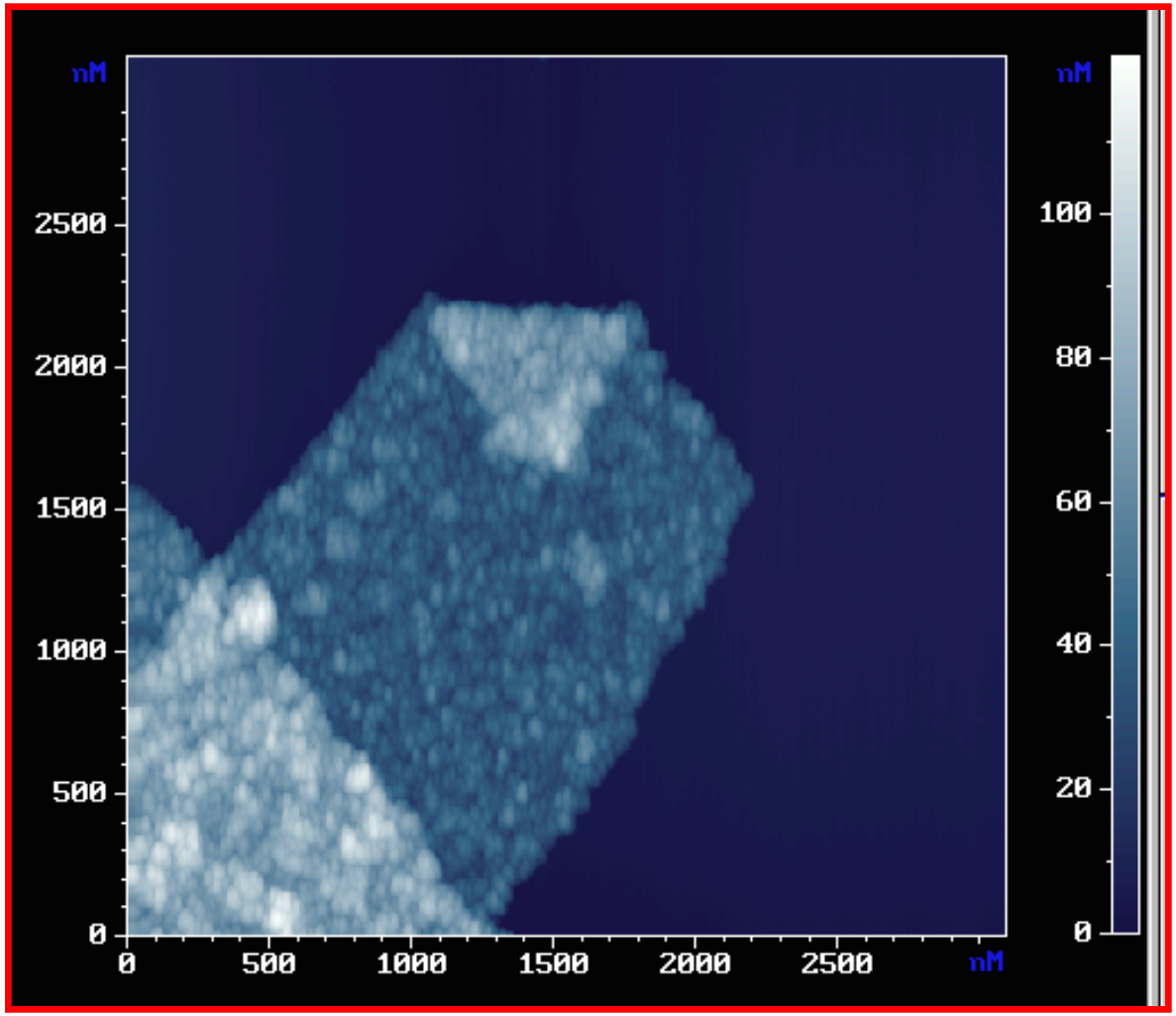

b

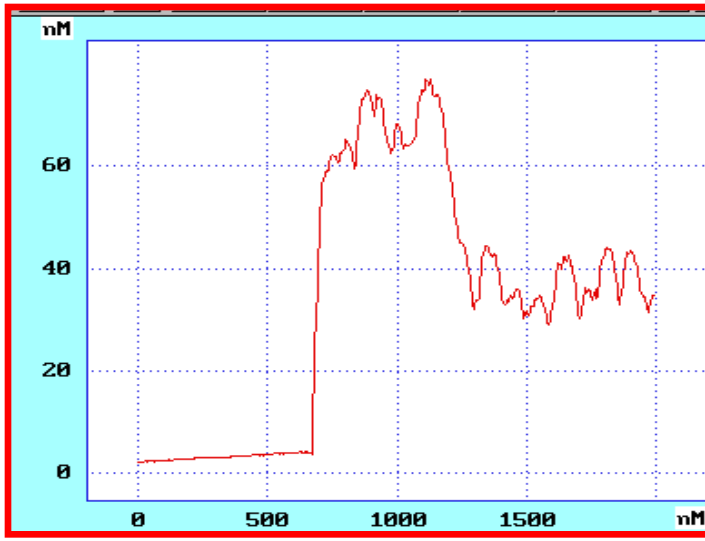

a): Topographyc image

b): Vertical cross-section profile

TEM micrographs of self-assembled nanofilm material

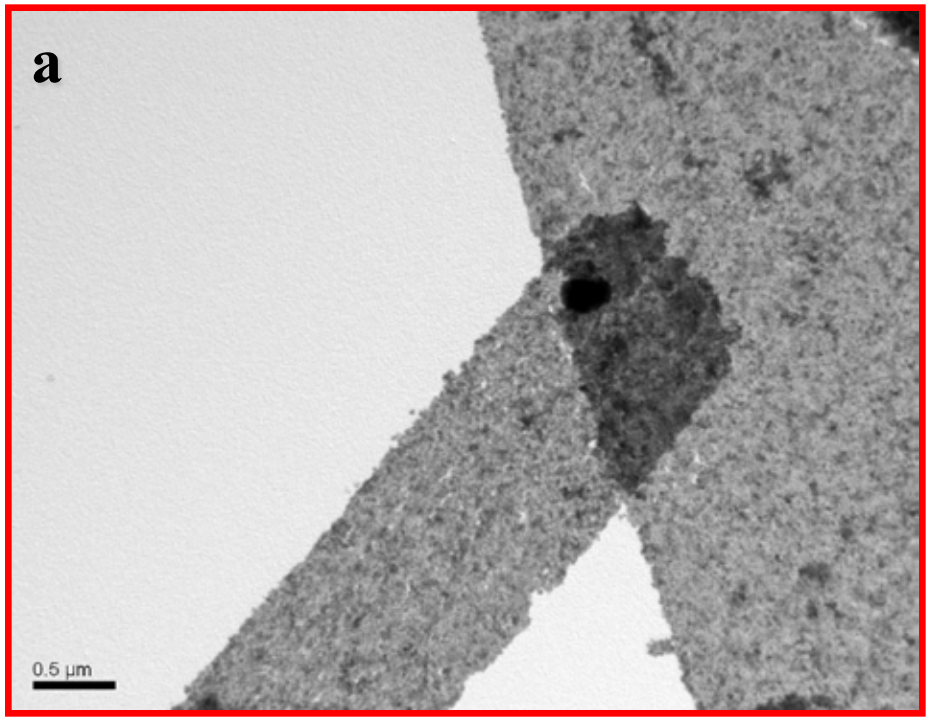

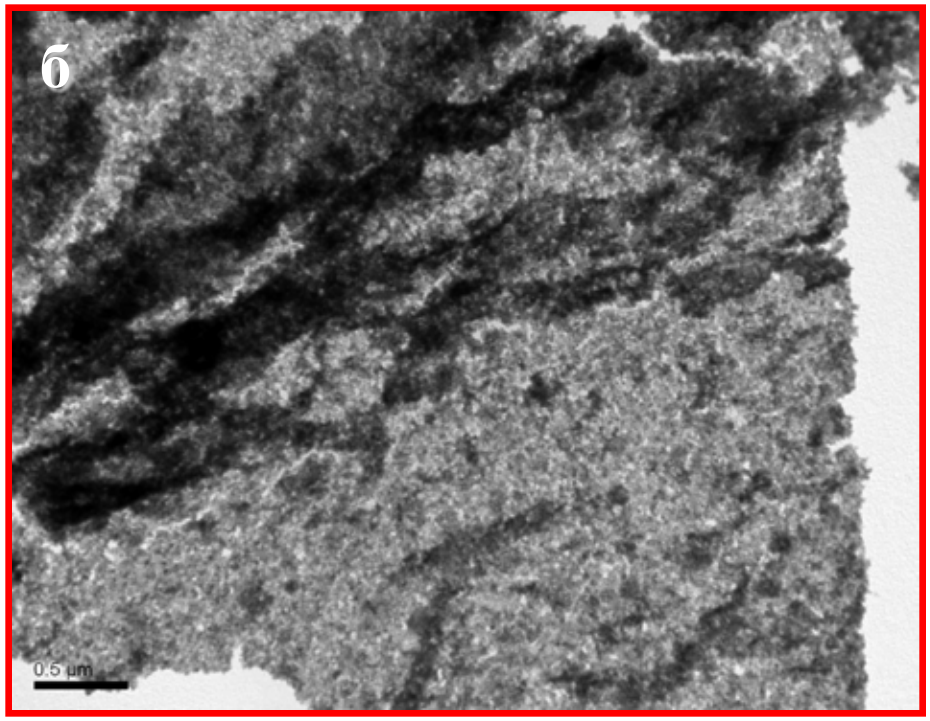

Nanoparticulate structures with different geometries, considered in theoretical modeling and calculations

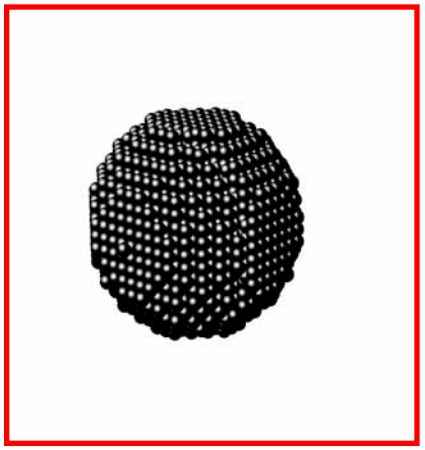

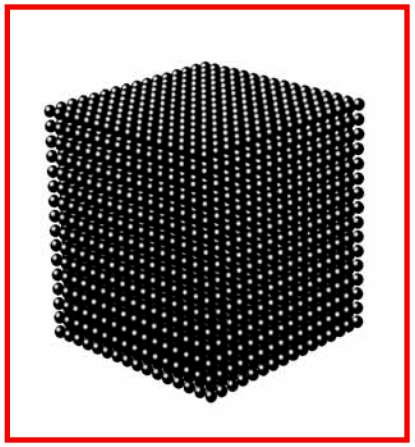

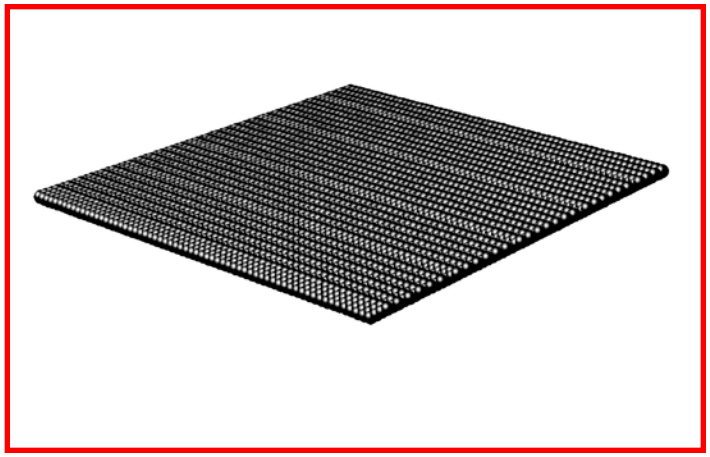

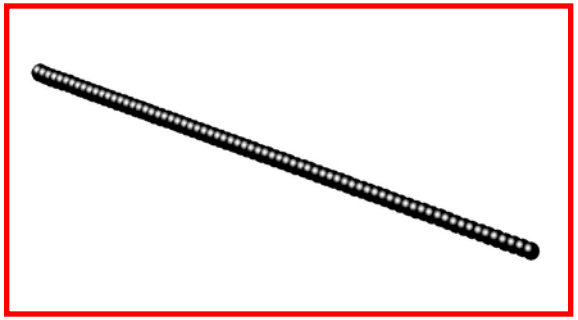

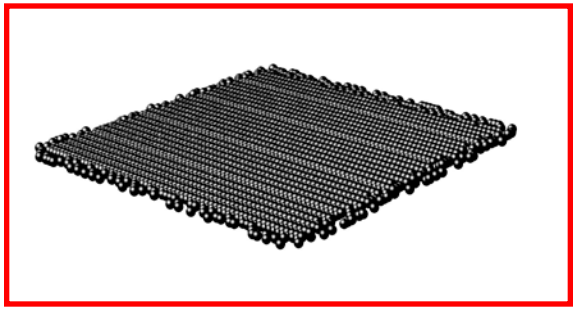

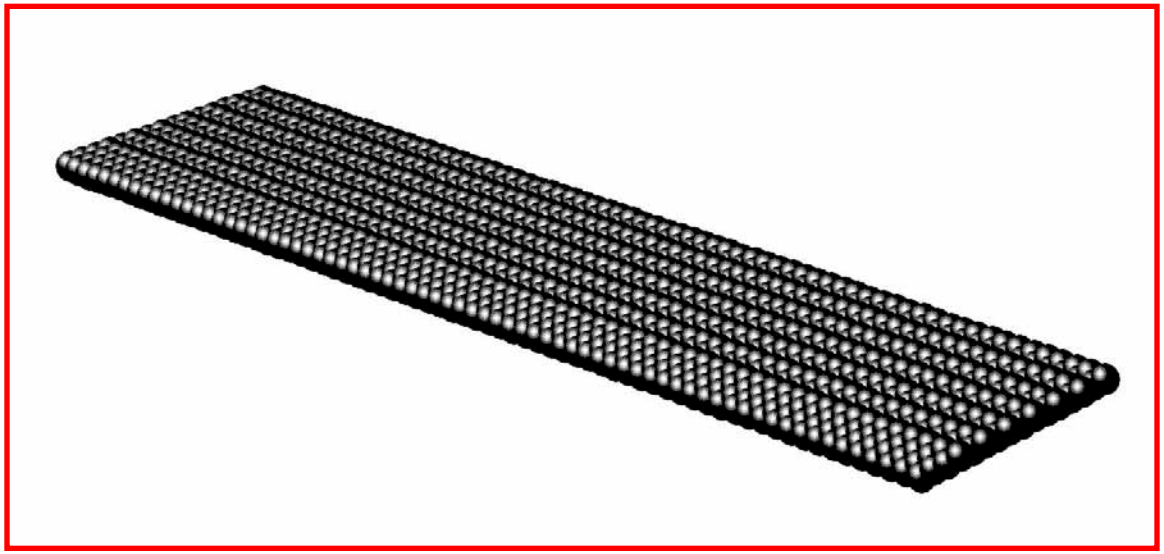

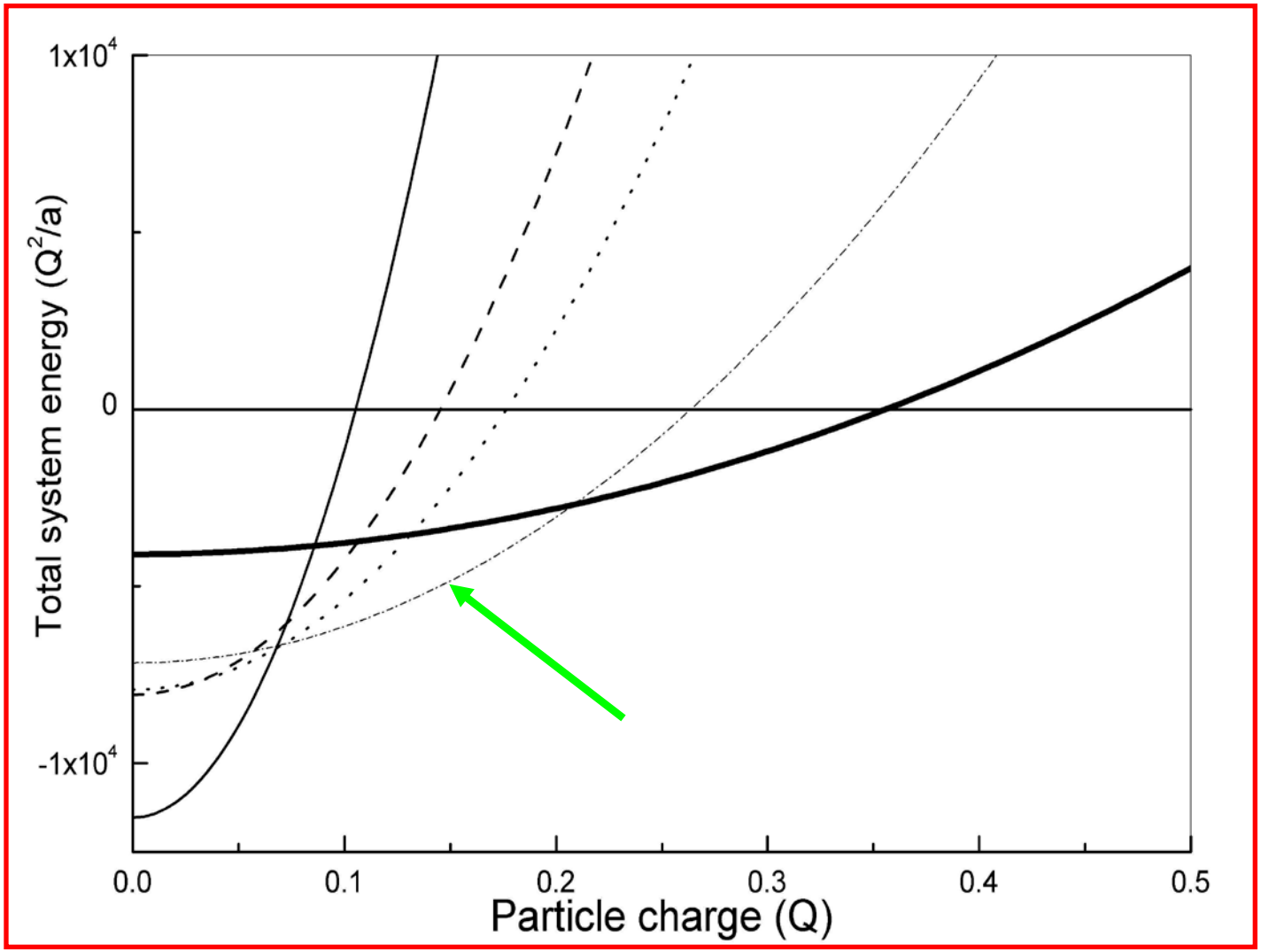

The sum energy of nanoparticulate systems as a function of the particle charge. Thin solid line – sphere, dashed line – planar square, dot line – rectangle with n=16, dashed-dot line - rectangle with n=256, thick line – linear structures (string). The distance between neighboring particles is unit (Q = 1, a = 1). The total particle number N = 4096.

TEM-image of the magnetic nanofilm material with bound colloid latex particles

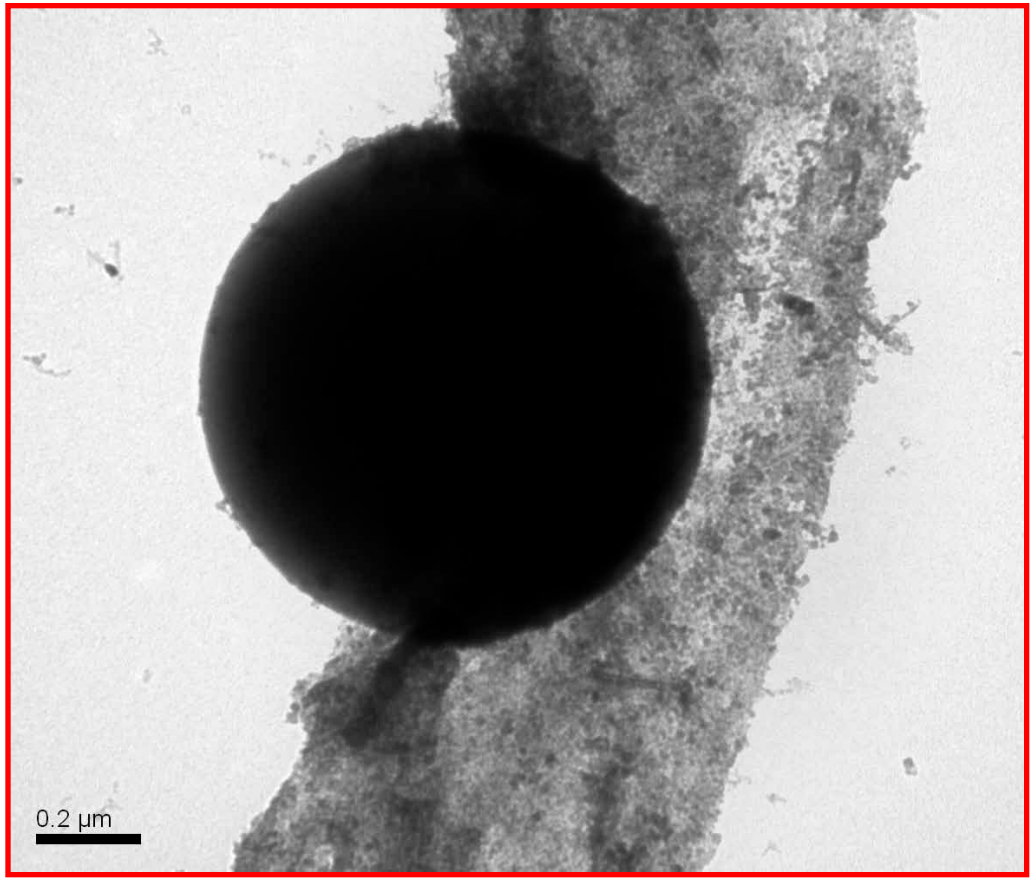

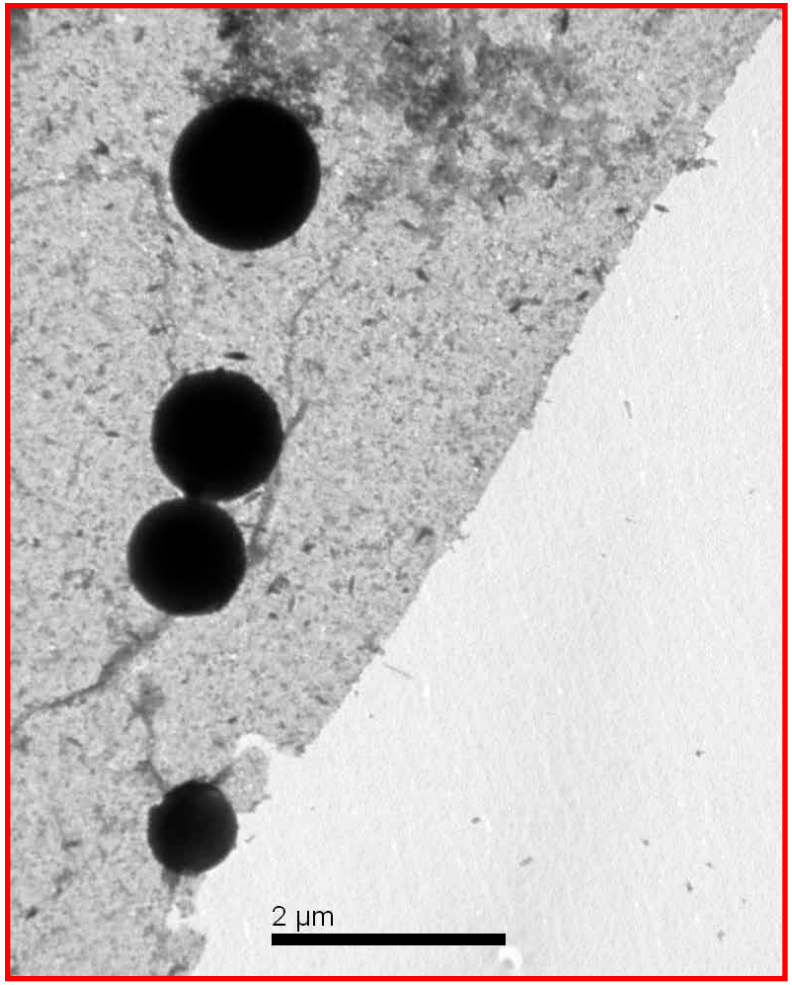

TEM-image of the magnetic nanofilm material deposited on surface of cotton fibers

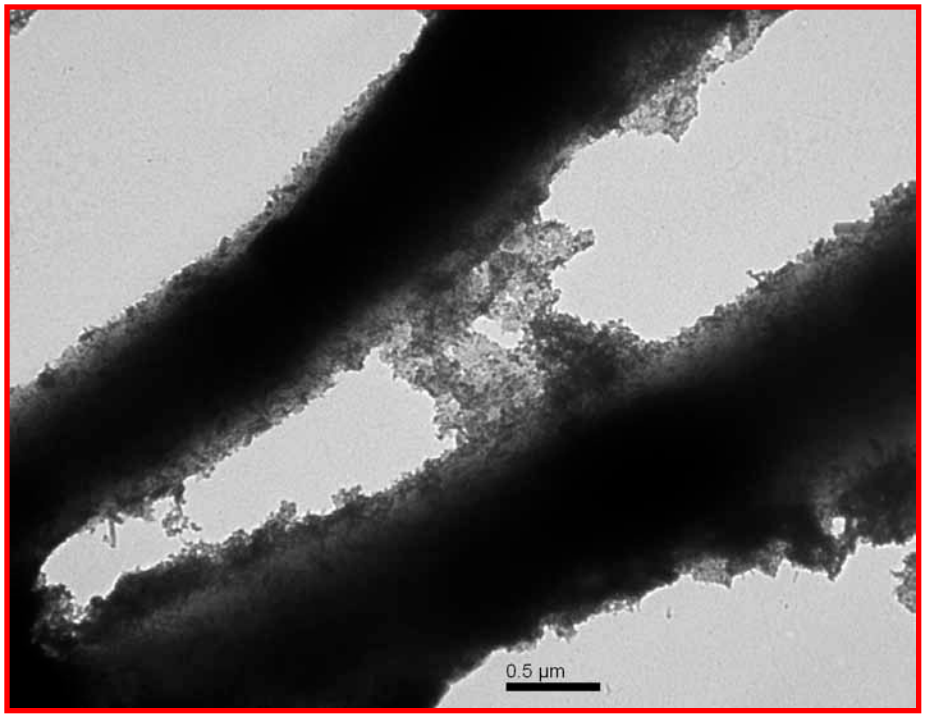

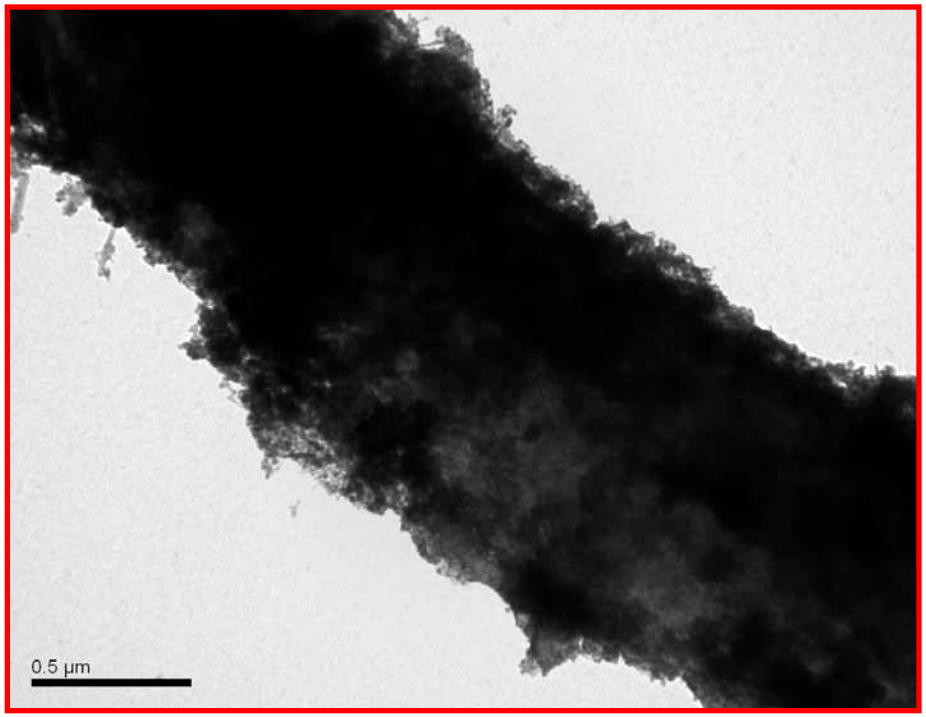

TEM images of sheet-like nanocomposite nanofilm material containing magnetic iron oxide nanoparticles and spermine interacting with bacteria

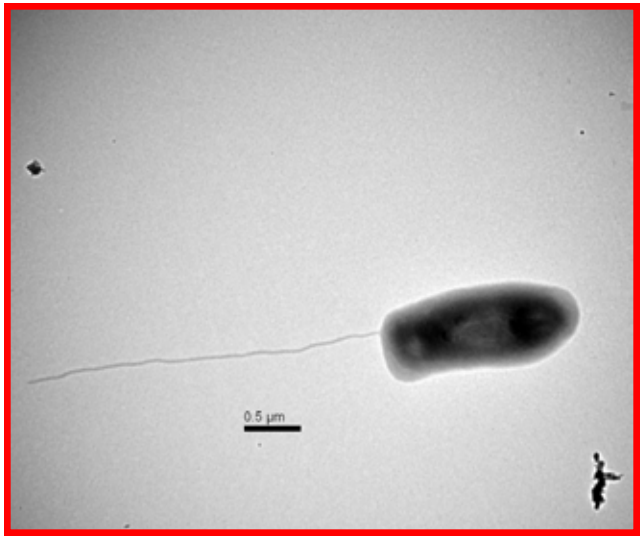

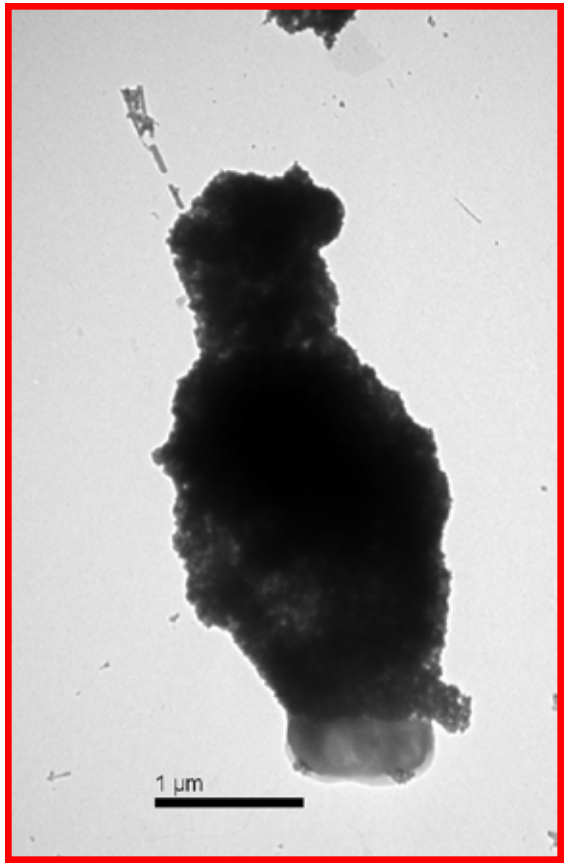

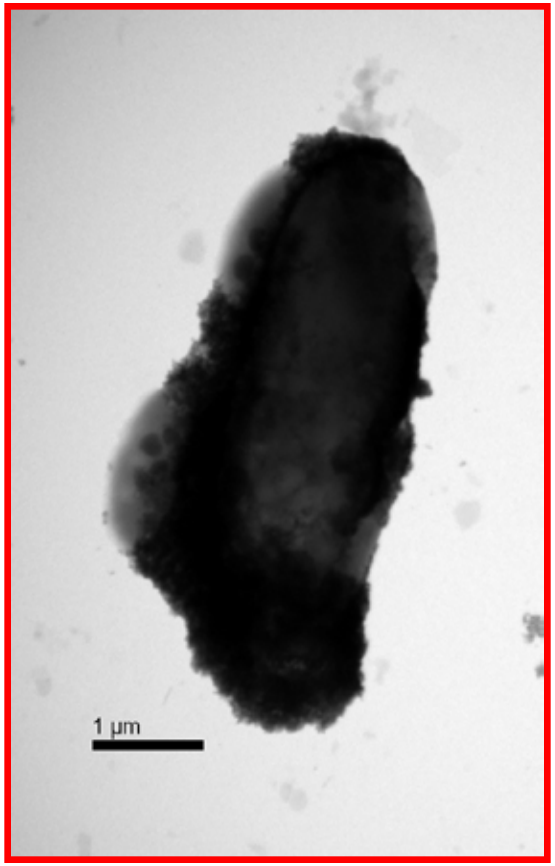

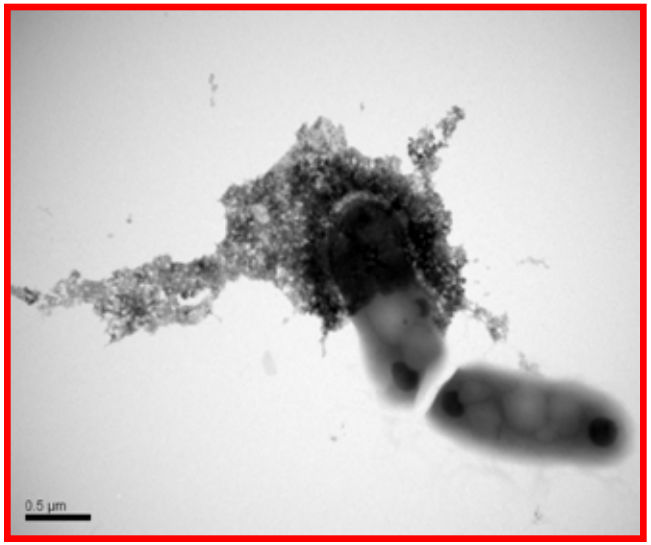

Conclusions

The data presented demonstrate the potential of methods based on combination of top-down and bottom-up approaches, scale integration, self-organization principles and ligand exchange and substitution reactions in DNA complexes for cost-effective nanofabrication of new nanoscale-organized hybrid bio-inorganic nanostructures.

The described synthetic strategies and methods are relatively simple, rapid, inexpensive and allow large-scale and parallel preparation of organized functional nanomaterials at ambient and ecologically-friendly conditions that makes them potentially promising for applications in a number of fields of modern materials science and nanobiotechnology, medicine….

Thank you for your attention!

Acknowledgements

AFM images were gratefully obtained by Dr. R.V. Gainutdinov and Dr. A.L. Tolstikhina, Institute of Crystallography RAS (Moscow). CdSe nanorods were synthesized by Dr. M. Artemyev (Institute for Physico-Chemical Problems, Belarussian State University, Minsk).

I thank to Prof. S.P. Gubin, Prof. V.V. Kislov, Prof. A.A. Yaroslavov, Dr. Yu.A. Koksharov, Dr. M. Artemyev, Dr. M.N. Antipina, Mr. A.N. Sergeev-Cherenkov, Dr. A.A. Rakhnyanskaya, Dr. A.V. Volkov, D.I. Chernichko for collaboration in experimental work and for discussions.

Contacts:

Gennady B. Khomutov,
E-mail: gbk@phys.msu.ru
gbk@mail.ru
Tel: +7 (495) 939-3025

$Fe^{2+} + H_2O_2 \rightarrow Fe^{3+} + {}^{\cdot}OH + OH^{-}$

$Fe^{3+} + H_2O_2 \rightarrow Fe^{2+} + O^{2-} + H^{+}$

$2H_2O_2 \xrightarrow{\text{катализатор Fe}} 2H_2O + O_2$

$O^{2-} + H_2O_2 \xrightarrow{\text{катализатор Fe}} O_2 + {}^{\cdot}OH + OH^{-}$